Full $H(\mathrm{div})-$Approximation of Linear Elasticity on Quadrilateral Meshes based on $\mathcal{ABF}$ Finite Elements

Thiago O. Quinelato[a,*], Abimael F. D. Loula[b], Maicon R. Correa[c], Todd Arbogast[d,e]

[a] *Universidade Federal de Juiz de Fora, Departamento de Matemática, Rua José Lourenço Kelmer, s/n, Campus Universitário, 36036-900 – Juiz de Fora, MG – Brazil*
[b] *Laboratório Nacional de Computação Científica, Av. Getúlio Vargas 333, 25651-075 – Petrópolis, RJ – Brazil*
[c] *Universidade Estadual de Campinas, Instituto de Matemática, Estatística e Computação Científica, Departamento de Matemática Aplicada, Rua Sérgio Buarque de Holanda, 651 Barão Geraldo, 13083-859 – Campinas, SP – Brazil*
[d] *Department of Mathematics, University of Texas, 2515 Speedway C1200, Austin, TX 78712-1202 – USA*
[e] *Institute for Computational Engineering and Sciences, University of Texas, 201 EAST 24th St. C0200, Austin, TX – 78712-1229 – USA*

Abstract

For meshes of nondegenerate, convex quadrilaterals, we present a family of stable mixed finite element spaces for the mixed formulation of planar linear elasticity. The problem is posed in terms of the stress tensor, the displacement vector and the rotation scalar fields, with the symmetry of the stress tensor weakly imposed. The proposed spaces are based on the Arnold-Boffi-Falk ($\mathcal{ABF}_k$, $k \geq 0$) elements for the stress and piecewise polynomials for the displacement and the rotation. We prove that these finite elements provide full $H(\mathrm{div})-$approximation of the stress field, in the sense that it is approximated to order h^{k+1}, where h is the mesh diameter, in the $H(\mathrm{div})-$norm. We show that displacement and rotation are also approximated to order h^{k+1} in the L^2-norm. The convergence is optimal order for $k \geq 1$, while the lowest order case, index $k = 0$, requires special treatment. The spaces also apply to both compressible and incompressible isotropic problems, i.e., the Poisson ratio may be one-half. The implementation as a hybrid method is discussed, and numerical results are given to illustrate the effectiveness of these finite elements.

Keywords: Linear elasticity, Mixed finite element method, Quadrilateral element, Full $H(\mathrm{div})$-approximation, Hybrid formulation

1. Introduction

Let Ω be a planar region occupied by a linear elastic body. The general form of the linear elasticity problem consists of the linear constitutive equation, which relates the deformation suffered by an elastic body to its stress state (Arnold, 1990),

$$\boldsymbol{A}\boldsymbol{\sigma} = \boldsymbol{\varepsilon}(\boldsymbol{u}) \quad \text{in } \Omega, \tag{1}$$

and the equilibrium equation, which states the conservation of linear momentum,

$$\operatorname{div} \boldsymbol{\sigma} = \boldsymbol{g} \quad \text{in } \Omega, \tag{2}$$

*Corresponding author
Email addresses: thiago.quinelato@ice.ufjf.br (Thiago O. Quinelato), aloc@lncc.br (Abimael F. D. Loula), maicon@ime.unicamp.br (Maicon R. Correa), arbogast@ices.utexas.edu (Todd Arbogast)

where $\boldsymbol{u} : \Omega \to \mathbb{R}^2$ is the displacement field, $\boldsymbol{\varepsilon}(\boldsymbol{u})$ is the corresponding infinitesimal strain tensor, given by the symmetric part of the gradient of $\boldsymbol{u}$,

$$\boldsymbol{\varepsilon}(\boldsymbol{u}) = \nabla^s \boldsymbol{u} = \frac{1}{2}\Big(\nabla \boldsymbol{u} + (\nabla \boldsymbol{u})^t\Big),$$

$\boldsymbol{g}$ denotes the imposed volume load and $\boldsymbol{\sigma} : \Omega \to \mathbb{S}$, where $\mathbb{S} = \mathbb{R}^{2\times 2}_{\text{sym}}$ is the space of symmetric second order real tensors, is the stress field. For simplicity, we only consider prescribed displacement $\boldsymbol{u} = \boldsymbol{u}_{\text{B}}$ on the boundary $\Gamma = \partial\Omega$, although other boundary conditions could be handled in the usual ways. The divergence operator div applies to the matrix field $\boldsymbol{\sigma}$ row-by-row. The material properties are determined by the compliance tensor $\boldsymbol{A}$, which is a positive definite symmetric operator from $\mathbb{S}$ to itself, possibly depending on the point $\boldsymbol{x} \in \Omega$. In the isotropic case it is given by

$$\boldsymbol{A}\boldsymbol{\sigma} = \frac{1}{2\mu}\left(\boldsymbol{\sigma} - \frac{\lambda}{2(\lambda+\mu)}\operatorname{tr}(\boldsymbol{\sigma})\boldsymbol{I}\right), \tag{3}$$

where $\lambda \geq 0$ and $\mu > 0$ are the Lamé constants and $\boldsymbol{I}$ denotes the identity tensor. The inverse of $\boldsymbol{A}$ is the elasticity tensor $\boldsymbol{C} : \mathbb{S} \to \mathbb{S}$, that in the isotropic case is given by

$$\boldsymbol{C}\boldsymbol{\varepsilon} = 2\mu\boldsymbol{\varepsilon} + \lambda \operatorname{tr}(\boldsymbol{\varepsilon})\boldsymbol{I} = \boldsymbol{\sigma}.$$

Although this problem has already been the focus of many studies, there are still numerous challenges in the development of numerical and computational methods that are capable of providing stable and accurate solutions, especially on quadrilaterals and hexahedra. The elliptic equation posed on displacements only,

$$\operatorname{div}\big(\boldsymbol{C}\boldsymbol{\varepsilon}(\boldsymbol{u})\big) = \boldsymbol{g} \quad \text{in } \Omega, \tag{4}$$

found by inverting the compliance tensor in (1) and substituting the stress in (2), is the basis for the definition of the standard primal Galerkin method (Arnold, 1990). This standard method is suitable for compressible problems. For incompressible problems, however, as the Poisson ratio $\nu = \lambda/2(\lambda+\mu)$ approaches 0.5 (i.e., $\lambda \to \infty$), the elasticity tensor $\boldsymbol{C}$ becomes infinite, and a mixed formulation must be employed to solve (1)–(2).

1.1. Mixed Formulations

One of the great advantages of mixed formulations for the elasticity problem is the possibility of obtaining conservative solutions with balanced convergence order for stress and displacement fields. Moreover, they are robust in the incompressible limit, not being subject to the volumetric locking effect (Arnold, 1990; Loula et al., 1987; Stein & Rolfes, 1990; Oyarzúa & Ruiz-Baier, 2016). In general, mixed formulations for the elasticity problem seek for the simultaneous evaluation of the pair $(\boldsymbol{\sigma}, \boldsymbol{u})$ (Amara & Thomas, 1979; Mignot & Surry, 1981; Arnold et al., 1984,; Stenberg, 1986, 1988,; Arnold & Winther, 2002; Adams & Cockburn, 2005; Arnold & Awanou, 2005; Arnold et al., 2007; Gatica, 2007; Arnold et al., 2015). This pair can be characterized as the unique solution of the Hellinger-Reissner functional or, equivalently, as the unique solution of the following weak formulation: *Find* $(\boldsymbol{\sigma}, \boldsymbol{u}) \in H(\operatorname{div}, \Omega, \mathbb{S}) \times L^2(\Omega, \mathbb{R}^2)$ *such that*

$$(\boldsymbol{A}\boldsymbol{\sigma}, \boldsymbol{\tau}) + (\boldsymbol{u}, \operatorname{div}\boldsymbol{\tau}) = \langle \boldsymbol{u}_{\text{B}}, \boldsymbol{\tau}\boldsymbol{\nu}\rangle_\Gamma \quad \forall \boldsymbol{\tau} \in H(\operatorname{div}, \Omega, \mathbb{S}), \tag{5a}$$

$$(\operatorname{div}\boldsymbol{\sigma}, \boldsymbol{\eta}) = (\boldsymbol{g}, \boldsymbol{\eta}) \quad \forall \boldsymbol{\eta} \in L^2(\Omega, \mathbb{R}^2), \tag{5b}$$

where $H(\operatorname{div}, \Omega, \mathbb{S})$ is the space of square-integrable symmetric matrix fields with square-integrable divergence, $L^2(\Omega, \mathbb{R}^2)$ is the space of square-integrable vector fields, $(\cdot,\cdot)$ denotes the $L^2(\Omega, \mathbb{R}^2)$ or $L^2(\Omega, \mathbb{R}^{2\times 2})$ inner product and $\langle\cdot,\cdot\rangle_\Gamma$ denotes the $L^2(\Gamma, \mathbb{R}^2)$ inner product (or duality pairing). Later we will restrict the domain of integration to a measurable set $K \subset \Omega$ by writing $(\cdot,\cdot)_K$, or by changing Γ to another space of dimension one.

To demonstrate the stability of a mixed formulation, one usually relies on the satisfaction of the two hypotheses of Brezzi's theorem (Brezzi, 1974): the coercivity of a bilinear form and an inf-sup compatibility condition between the function spaces. In the context of linear elasticity, these conditions come together with other requirements, such as the conservation of angular momentum, characterized by the symmetry of the stress tensor. Indeed, the construction of finite element approximation strategies for the Hellinger-Reissner formulation that simultaneously satisfy the compatibility condition between the approximation spaces and the restriction of symmetry of the stress tensor is not trivial (Arnold & Winther, 2002; Arnold & Awanou, 2005; Adams & Cockburn, 2005).

The first strategies for approximating the elasticity problem in the mixed form were based on the exact enforcement of the symmetry of the stress tensor in the construction of the approximation space. In this direction, are the composite finite element methods (Watwood Jr & Hartz, 1968; Johnson & Mercier, 1978; Arnold et al., 1984; Zienkiewicz, 2001). The first mixed finite element methods with polynomial approximation of the symmetric stress tensor and of the displacement field were presented in the 2000's (Arnold & Winther, 2002; Adams & Cockburn, 2005; Arnold et al., 2008). These finite elements tend to have a high number of degrees of freedom. The lowest order approximation is based on cubic polynomials for each component of the tensor and linear polynomials for each component of the vector. The approximated stresses are continuous, while the displacements are discontinuous. An alternative way of approximating the mixed formulation is to relax the $H(\mathrm{div})-$conformity of the stress approximation and to preserve the symmetry (Arnold & Winther, 2003; Awanou, 2009; Hu & Shi, 2007; Man et al., 2009; Yi, 2005, 2006; Gopalakrishnan & Guzmán, 2011).

Another approach, which we take in this paper, is to use a modified variational formulation, aiming to approximate the stress tensor in $H(\mathrm{div}, \Omega, \mathbb{M})$, where $\mathbb{M} = \mathbb{R}^{2\times 2}$ is the space of second order real tensors (Amara & Thomas, 1979; Mignot & Surry, 1981; Arnold et al., 1984; Stenberg, 1986, 1988,; Arnold & Falk, 1988; Morley, 1989; Stein & Rolfes, 1990; Farhloul & Fortin, 1997; Arnold et al., 2006, 2007; Boffi et al., 2009; Qiu & Demkowicz, 2009; Cockburn et al., 2010; Guzmán, 2010; Gopalakrishnan & Guzmán, 2012; Gatica, 2014). In general, these formulations maintain exact $H(\mathrm{div})-$conformity, but impose the symmetry condition only in a weak sense. This is often done via the introduction of a Lagrange multiplier that is related to the rotation (see Section 2). This idea was first suggested by Fraeijs de Veubeke (1975) and has been applied in various works (Amara & Thomas, 1979; Arnold et al., 1984, 2006; Cockburn et al., 2010; Arnold et al., 2015).

1.2. Approximation on Quadrilateral Meshes

Mixed finite element methods for the elasticity problem on rectangular quadrilaterals and hexahedra have been proposed, e.g. in Yi (2005, 2006); Hu & Shi (2007); Man et al. (2009); Arnold et al. (2015). In this paper, we focus our attention on meshes of convex quadrilaterals. When compared to simplicial elements, quadrilaterals and hexahedra generate significantly fewer degrees of freedom (especially in the three-dimensional case or when the degrees of freedom associated with the rotation are local and can all be statically condensed). Also, a logically rectangular indexing can be applied to fairly general quadrilateral meshes, or at least for patches of meshes, which contributes to reduce the coding effort and run-time.

To the extent of our knowledge, there is currently no conforming mixed finite element method for the Hellinger-Reissner formulation that provides an approximation on arbitrary convex quadrilateral meshes that simultaneously enforces the conservation of linear and angular momenta with $\mathcal{O}(h^{k+1})$ convergence for the stress field in the $H(\mathrm{div})-$norm, i.e., that has full $H(\mathrm{div})-$approximation. We will provide such a full $H(\mathrm{div})-$approximating element in this paper. Here we use the terminology of Arbogast & Correa (2016), where finite element subspaces of $H(\mathrm{div}) \times L^2$ for the Poisson problem are classified as having either full $H(\mathrm{div})-$approximation, where the flux, the potential and the divergence of the flux are approximated to the same order (like the Raviart-Thomas, $\mathcal{RT}_k$, elements of index $k \geq 0$ (Raviart & Thomas, 1977)) or reduced $H(\mathrm{div})-$approximation, where the potential and the divergence of the flux are approximated to one less power (like the Brezzi-Douglas-Marini, $\mathcal{BDM}_k$, elements of

index $k \geq 1$ (Brezzi et al., 1985)).

Two mixed methods with weakly imposed symmetry on quadrilateral meshes were introduced by Arnold et al. (2015). Their first choice of spaces uses a product of $\mathcal{RT}_k$ spaces, $k \geq 1$, on quadrilaterals to approximate the stress, mapped tensor product polynomials to approximate each component of the displacement and unmapped polynomials (defined directly in the coordinates of the element K) to approximate the rotation. On meshes formed by parallelograms, the approximations show full $H(\mathrm{div})-$approximation, i.e., $\mathcal{O}(h^{k+1})$ convergence rates for the stress in the $H(\mathrm{div}, \Omega, \mathbb{M})$ norm, for the displacement in the $L^2(\Omega, \mathbb{R}^2)$ norm and for the rotation in the $L^2(\Omega, \mathbb{R})$ norm. However, on meshes with arbitrary quadrilaterals, this choice is unable to provide $\mathcal{O}(h^{k+1})$ convergence for the stress in the $H(\mathrm{div}, \Omega, \mathbb{M})$ seminorm, i.e., of the divergence of the stress. The convergence is $\mathcal{O}(h^k)$, so we should consider these spaces as being a reduced $H(\mathrm{div})-$approximation family.

Their second choice of spaces is based on the $\mathcal{BDM}_k$ spaces. The lowest order spaces in this family ($k = 1$) require a piecewise constant approximation for each component of the displacement vector. In this case, the rotation is also sought in a space of piecewise constant functions. When meshes of parallelograms are used, the convergence rates for the $\mathcal{BDM}_1-$based spaces are $\mathcal{O}(h)$ for all three variables. In the case of general quadrilateral meshes, the approximation of the stress field does not converge in the $H(\mathrm{div}, \Omega, \mathbb{M})$ seminorm.

The shortcoming of the above two spaces is due to the fact that both $\mathcal{RT}_k$ and $\mathcal{BDM}_k$ do not provide $\mathcal{O}(h^{k+1})$ approximations of divergences on non-parallelogram meshes, as was studied by Arnold et al. (2005). In this same work, the authors present necessary conditions for $\mathcal{O}(h^{k+1})$ approximations of vector fields on quadrilaterals, both in the L^2 and $H(\mathrm{div})$ norms. They also introduce a family of spaces satisfying these conditions: the Arnold-Boffi-Falk, $\mathcal{ABF}_k$, spaces of index $k \geq 0$.

As our main contribution, we introduce a family of approximation spaces with weakly imposed symmetry that provides full $H(\mathrm{div})-$approximation for index $k \geq 0$, and gives optimal order convergence for $k \geq 1$, even on arbitrary convex quadrilaterals. Moreover, our spaces preserve the continuity of the traction across interelement edges. The spaces for the stress-displacement pair are based on the $\mathcal{ABF}_k$ elements. The Lagrange multiplier associated with the symmetry of the stress tensor is approximated by a piecewise polynomial function with no continuity restriction. Thus, the associated degrees of freedom can be condensed in a hybridization process, and the introduction of the Lagrange multiplier to enforce the symmetry condition (and consequently the conservation of angular momentum) does not affect the size of the global linear system of equations resulting from the discretization. Furthermore, the adoption of a hybrid strategy facilitates the construction of local bases for the approximation spaces and allows for the elimination of all local degrees of freedom.

The text is organized as follows. We present the mixed formulation with weakly imposed symmetry in the next section. Its finite element approximation is commented on in Section 3, where we review the theory of stability given by Arnold et al. (2015). The $\mathcal{ABF}-$based full $H(\mathrm{div})-$approximating spaces are defined in Section 4. The lowest order case $k = 0$ does not maintain stability, and so requires special treatment. We introduce two new low order finite elements that remain stable and have local dimension smaller than the lowest known $\mathcal{RT}_1-$based element. The error in the approximation is analyzed in Section 5. We also introduce a stabilizing term into the formulation to handle the lowest order case. Implementation using the hybrid form of the method is described in Section 6, and numerical results are presented in Section 7. Conclusions are given in the last section of the paper, where the convergence order and the degrees of freedom of the spaces are summarized (see Table 6).

2. The Mixed Formulation with Weakly Imposed Symmetry

We denote by $H^k(T, X)$ the Sobolev space consisting of functions with domain $T \subset \mathbb{R}^2$, taking values in the finite-dimensional vector space X, and with all derivatives of order at most k square integrable. We similarly denote by $\mathbb{P}_k(T, X)$ the space of polynomial functions on T of degree at most k taking values in X, and by $\mathbb{P}_{k_1,k_2}(T, X)$

the space of polynomial functions on T of degree at most $k_1 \geq 0$ in $x = x_1$ and degree at most $k_2 \geq 0$ in $y = x_2$, taking values in X. The range space X will be either $\mathbb{R}$, $\mathbb{R}^2$ or $\mathbb{M} = \mathbb{R}^{2\times 2}$.

We seek approximations for the stress field in $H(\mathrm{div}, \Omega, \mathbb{M})$ and introduce the symmetry condition in the variational sense (Fraeijs de Veubeke, 1975; Arnold et al., 1984, 2006, 2007). We add a third variable to the problem, a Lagrange multiplier associated to the rotation and defined as

$$r(\boldsymbol{u}) = \mathrm{asym}(\nabla \boldsymbol{u})/2,$$

where

$$\mathrm{asym}\, \boldsymbol{\tau} = \boldsymbol{\tau}_{12} - \boldsymbol{\tau}_{21}$$

is a measure of the asymmetry of the matrix $\boldsymbol{\tau} \in \mathbb{M}$, and rewrite the constitutive equation (1) as

$$\boldsymbol{A}\boldsymbol{\sigma} = \nabla \boldsymbol{u} - \boldsymbol{R}, \tag{6}$$

with

$$\boldsymbol{R} = r \begin{bmatrix} 0 & 1 \\ -1 & 0 \end{bmatrix}.$$

Recall that $\boldsymbol{A}$ is defined in (3), and define

$$\mathcal{S} = H(\mathrm{div}, \Omega, \mathbb{M}), \quad \mathcal{U} = L^2(\Omega, \mathbb{R}^2), \quad \mathcal{R} = L^2(\Omega, \mathbb{R}).$$

The modified mixed formulation for the elasticity problem is: *Given* $\boldsymbol{u}_\mathrm{B} \in H^{1/2}(\Gamma, \mathbb{R}^2)$ *and* $\boldsymbol{g} \in L^2(\Omega, \mathbb{R}^2)$*, find* $(\boldsymbol{\sigma}, \boldsymbol{u}, r) \in \mathcal{S} \times \mathcal{U} \times \mathcal{R}$ *satisfying*

$$(\boldsymbol{A}\boldsymbol{\sigma}, \boldsymbol{\tau}) + (\boldsymbol{u}, \mathrm{div}\, \boldsymbol{\tau}) + (r, \mathrm{asym}\, \boldsymbol{\tau}) = \langle \boldsymbol{u}_\mathrm{B}, \boldsymbol{\tau}\boldsymbol{\nu} \rangle_\Gamma \quad \forall \boldsymbol{\tau} \in \mathcal{S}, \tag{7a}$$

$$(\mathrm{div}\, \boldsymbol{\sigma}, \boldsymbol{\eta}) = (\boldsymbol{g}, \boldsymbol{\eta}) \quad \forall \boldsymbol{\eta} \in \mathcal{U}, \tag{7b}$$

$$(\mathrm{asym}\, \boldsymbol{\sigma}, s) = 0 \quad \forall s \in \mathcal{R}. \tag{7c}$$

Note that $\boldsymbol{\tau}\boldsymbol{\nu} \in H^{-1/2}(\Gamma, \mathbb{R}^2)$. This variational form is constructed from the differential equations as follows. Taking the inner product of each term in (6) with a tensor $\boldsymbol{\tau} \in H(\mathrm{div}, \Omega, \mathbb{M})$, integrating in Ω and applying integration by parts to one of the terms, we have (7a). Similarly, taking the inner product of the equilibrium equation (2) with a vector $\boldsymbol{\eta} \in L^2(\Omega, \mathbb{R}^2)$ and integrating in Ω, one arrives at (7b). Equation (7c) imposes the symmetry condition on the stress tensor, in a variational sense.

The well-posedness of (7) is presented in Arnold et al. (2015) by using Brezzi's theory (Brezzi, 1974). In particular, the authors prove the following inf-sup condition.

Lemma 2.1: *There exists a constant* $\beta > 0$ *such that*

$$\inf_{\substack{\boldsymbol{u}\in\mathcal{U} \\ r\in\mathcal{R}}} \sup_{\boldsymbol{\tau}\in\mathcal{S}} \frac{(\mathrm{div}\, \boldsymbol{\tau}, \boldsymbol{u}) + (\mathrm{asym}\, \boldsymbol{\tau}, r)}{\|\boldsymbol{\tau}\|_\mathcal{S} \left(\|\boldsymbol{u}\|_\mathcal{U} + \|r\|_\mathcal{R} \right)} \geq \beta > 0.$$

Note that

$$\|\boldsymbol{\tau}\|_\mathcal{S} = \left(\|\boldsymbol{\tau}\|^2_{L^2} + \|\mathrm{div}\, \boldsymbol{\tau}\|^2_{L^2} \right)^{1/2}, \quad \|\boldsymbol{u}\|_\mathcal{U} = \|\boldsymbol{u}\|_{L^2}, \quad \|r\|_\mathcal{R} = \|r\|_{L^2}.$$

3. Finite Element Approximation and Stability

The discrete counterpart of the elasticity problem (7) is stated as follows.

Discrete Elasticity Problem: *Given* $\boldsymbol{u}_{\mathrm{B}} \in H^{1/2}(\Gamma, \mathbb{R}^2)$ *and* $\boldsymbol{g} \in L^2(\Omega, \mathbb{R}^2)$*, find the finite dimensional approximations* $(\boldsymbol{\sigma}_h, \boldsymbol{u}_h, r_h) \in \mathcal{S}_h \times \mathcal{U}_h \times \mathcal{R}_h$ *satisfying*

$$(\boldsymbol{A}\boldsymbol{\sigma}_h, \boldsymbol{\tau}_h) + (\boldsymbol{u}_h, \operatorname{div} \boldsymbol{\tau}_h) + (r_h, \operatorname{asym} \boldsymbol{\tau}_h) = \langle \boldsymbol{u}_{\mathrm{B}}, \boldsymbol{\tau}_h \boldsymbol{\nu} \rangle_{\Gamma} \quad \forall \boldsymbol{\tau}_h \in \mathcal{S}_h, \tag{8a}$$

$$(\operatorname{div} \boldsymbol{\sigma}_h, \boldsymbol{\eta}_h) = (\boldsymbol{g}, \boldsymbol{\eta}_h) \quad \forall \boldsymbol{\eta}_h \in \mathcal{U}_h, \tag{8b}$$

$$(\operatorname{asym} \boldsymbol{\sigma}_h, s_h) = 0 \quad \forall s_h \in \mathcal{R}_h, \tag{8c}$$

with $\boldsymbol{A}$ *as defined in* (3)*. The finite dimensional spaces* $\mathcal{S}_h$*,* $\mathcal{U}_h$ *and* $\mathcal{R}_h$ *are yet to be defined.*

The theory of stability of the solution of the Discrete Elasticity Problem was also developed by Arnold et al. (2015). It relies on the discrete counterpart of Brezzi's theorem (Brezzi, 1974), which requires the existence of positive constants α_E, β_E such that

$$(\boldsymbol{A}\boldsymbol{\tau}_h, \boldsymbol{\tau}_h) \geq \alpha_E \|\boldsymbol{\tau}_h\|_{\mathcal{S}}^2 \quad \forall \boldsymbol{\tau}_h \in \ker B_h, \tag{9}$$

$$\inf_{\substack{\boldsymbol{u}_h \in \mathcal{U}_h \\ r_h \in \mathcal{R}_h}} \sup_{\boldsymbol{\tau}_h \in \mathcal{S}_h} \frac{(\operatorname{div} \boldsymbol{\tau}_h, \boldsymbol{u}_h) + (\operatorname{asym} \boldsymbol{\tau}_h, r_h)}{\|\boldsymbol{\tau}_h\|_{\mathcal{S}} \left(\|\boldsymbol{u}_h\|_{\mathcal{U}} + \|r_h\|_{\mathcal{R}}\right)} \geq \beta_E > 0, \tag{10}$$

where

$$\ker B_h = \left\{ \boldsymbol{\tau}_h \in \mathcal{S}_h ; (\operatorname{div} \boldsymbol{\tau}_h, \boldsymbol{u}_h) + (\operatorname{asym} \boldsymbol{\tau}_h, r_h) = 0 \; \forall (\boldsymbol{u}_h, r_h) \in \mathcal{U}_h \times \mathcal{R}_h \right\}.$$

If we can take $\boldsymbol{\tau}_h = \boldsymbol{I}$ in (8a), i.e., if $\boldsymbol{I} \in \mathcal{S}_h$, it is possible to show that the constant α_E does not depend on λ (see Arnold et al. (1984) or Boffi et al. (2013)). This fact is crucial to the stability of the approximation in the incompressible limit (when $\lambda \to \infty$).

If Brezzi's conditions (9) and (10) are met (Arnold et al., 2015), there exists a positive constant γ_E (depending on α_E and β_E, but independent of h and λ) such that, for each choice $(\boldsymbol{\sigma}_h, \boldsymbol{u}_h, r_h) \in \mathcal{S}_h \times \mathcal{U}_h \times \mathcal{R}_h$, there exist nonzero $(\boldsymbol{\tau}_h, \boldsymbol{\eta}_h, s_h) \in \mathcal{S}_h \times \mathcal{U}_h \times \mathcal{R}_h$ such that

$$\mathcal{A}((\boldsymbol{\sigma}_h, \boldsymbol{u}_h, r_h), (\boldsymbol{\tau}_h, \boldsymbol{\eta}_h, s_h)) \geq \gamma_E \left\|(\boldsymbol{\sigma}_h, \boldsymbol{u}_h, r_h)\right\|_E \left\|(\boldsymbol{\tau}_h, \boldsymbol{\eta}_h, s_h)\right\|_E, \tag{11}$$

where $\mathcal{A}$ is the bilinear form defined on $(\mathcal{S} \times \mathcal{U} \times \mathcal{R}) \times (\mathcal{S} \times \mathcal{U} \times \mathcal{R})$ by

$$\mathcal{A}((\tilde{\boldsymbol{\sigma}}, \tilde{\boldsymbol{u}}, \tilde{r}), (\boldsymbol{\tau}, \boldsymbol{\eta}, s)) := (\boldsymbol{A}\tilde{\boldsymbol{\sigma}}, \boldsymbol{\tau}) + (\tilde{\boldsymbol{u}}, \operatorname{div} \boldsymbol{\tau}) + (\tilde{r}, \operatorname{asym} \boldsymbol{\tau}) + (\operatorname{div} \tilde{\boldsymbol{\sigma}}, \boldsymbol{\eta}) + (\operatorname{asym} \tilde{\boldsymbol{\sigma}}, s)$$

and

$$\left\|(\tilde{\boldsymbol{\sigma}}, \tilde{\boldsymbol{u}}, \tilde{r})\right\|_E := \|\tilde{\boldsymbol{\sigma}}\|_{\mathcal{S}} + \|\tilde{\boldsymbol{u}}\|_{\mathcal{U}} + \|\tilde{r}\|_{\mathcal{R}}.$$

In summary, the following Theorem holds.

Theorem 3.1: *If* (9) *and* (10) *hold, then there is a unique solution to* (8) *and there is a constant* C*, independent of* h*, such that*

$$\left\|(\boldsymbol{\sigma}_h, \boldsymbol{u}_h, r_h)\right\|_E \leq C \left\{ \|\boldsymbol{u}_{\mathrm{B}}\|_{H^{1/2}(\Gamma, \mathbb{R}^2)} + \|\boldsymbol{g}\|_{L^2(\Omega, \mathbb{R}^2)} \right\}. \tag{12}$$

Moreover, if $\boldsymbol{I} \in \mathcal{S}_h$*, then* C *is independent of* λ*, and so* λ *may be taken as infinite, and* (11) *holds, provided that the globally constant mode for the trace of* $\boldsymbol{\sigma}$ *is removed.*

Arnold et al. (2015) also give a criterion for proving the inf-sup condition (10). It is based on the stability results for two auxiliary problems: the dual mixed form of the Poisson problem and the classical mixed form of the Stokes problem. We define $\operatorname{curl} \boldsymbol{w}$ for a vector field $\boldsymbol{w}$ as the matrix field whose first row is $\operatorname{curl} w_1$ and the second row is $\operatorname{curl} w_2$, where $\operatorname{curl} q = (\partial_2 q, -\partial_1 q)$ for a scalar function q.

Lemma 3.2: *Let $\mathcal{V}_h \subset H(\mathrm{div}, \Omega, \mathbb{R}^2)$ and $\mathcal{P}_h \subset L^2(\Omega, \mathbb{R})$ satisfy the inf-sup condition for the mixed Poisson problem, i.e., $\exists \beta_P > 0$ such that*

$$\sup_{\boldsymbol{v}_h \in \mathcal{V}_h} \frac{(\mathrm{div}\, \boldsymbol{v}_h, p_h)}{\|\boldsymbol{v}_h\|_{\mathcal{V}_h}} \geq \beta_P \|p_h\|_{\mathcal{P}_h} \quad \forall p_h \in \mathcal{P}_h. \tag{13}$$

Let $\mathcal{W}_h \subset H^1(\Omega, \mathbb{R}^2)$ and $\mathcal{R}_h \subset L^2(\Omega, \mathbb{R})$ satisfy the inf-sup condition for the Stokes problem, i.e., $\exists \beta_S > 0$ such that

$$\sup_{\boldsymbol{w}_h \in \mathcal{W}_h} \frac{(\mathrm{div}\, \boldsymbol{w}_h, r_h)}{\|\boldsymbol{w}_h\|_{\mathcal{W}_h}} \geq \beta_S \|r_h\|_{\mathcal{R}_h} \quad \forall r_h \in \mathcal{R}_h. \tag{14}$$

Finally, let $\mathcal{S}_h := \mathcal{V}_h \times \mathcal{V}_h$ be the space of matrices whose rows are composed by the transpose of vectors in $\mathcal{V}_h$. If

$$\mathrm{curl}\, \mathcal{W}_h \subset \mathcal{S}_h, \tag{15}$$

then $\mathcal{S}_h \subset H(\mathrm{div}, \Omega, \mathbb{M})$, $\mathcal{U}_h := \mathcal{P}_h \times \mathcal{P}_h \subset L^2(\Omega, \mathbb{R}^2)$ and $\mathcal{R}_h \subset L^2(\Omega, \mathbb{R})$ satisfy the discrete inf-sup condition (10).

4. $\mathcal{ABF}-$Based Full $H(\mathrm{div})-$Approximating Spaces

Let $\mathcal{T}_h$ be a conforming finite element mesh of nondegenerate, convex quadrilaterals K over the domain Ω of maximal diameter h. The $\mathcal{ABF}$ spaces (Arnold et al., 2005) are constructed by mapping polynomials defined on the reference element $\hat{K} = [-1, 1]^2$ to each element K of the mesh $\mathcal{T}_h$. We denote by $\boldsymbol{F}_K : \hat{K} \to K$ the invertible, bilinear map of the two domains in $\mathbb{R}^2$. A scalar-valued or vector-valued function $\hat{\varphi}$ on $\hat{K}$ transforms to a function $\varphi = P_K^0 \hat{\varphi}$ on K by the composition

$$\varphi(\boldsymbol{x}) = (P_K^0 \hat{\varphi})(\boldsymbol{x}) = \hat{\varphi}(\hat{\boldsymbol{x}}), \tag{16}$$

where $\boldsymbol{x} = \boldsymbol{F}_K(\hat{\boldsymbol{x}})$. A vector-valued function $\hat{\boldsymbol{\varphi}}$ on $\hat{K}$ transforms to a function $\boldsymbol{\varphi} = P_K^1 \hat{\boldsymbol{\varphi}}$ on K via the Piola transform

$$\boldsymbol{\varphi}(\boldsymbol{x}) = (P_K^1 \hat{\boldsymbol{\varphi}})(\boldsymbol{x}) = \frac{1}{J_K(\hat{\boldsymbol{x}})} [D\boldsymbol{F}_K(\hat{\boldsymbol{x}})] \hat{\boldsymbol{\varphi}}(\hat{\boldsymbol{x}}), \tag{17}$$

where $D\boldsymbol{F}_K(\hat{\boldsymbol{x}})$ is the Jacobian matrix of the mapping $\boldsymbol{F}_K$ and $J_K(\hat{\boldsymbol{x}})$ is its determinant. A matrix-valued function on $\hat{K}$ can be transformed onto K by applying the Piola transform (17) to each row. We also denote this operation by P_K^1.

The $\mathcal{ABF}$ space of index $k \geq 0$, $\mathcal{V}^k_{\mathcal{ABF}} \times \mathcal{P}^k_{\mathcal{ABF}}$, is defined to be

$$\mathcal{V}^k_{\mathcal{ABF}} = \{\boldsymbol{u}_h \in H(\mathrm{div}, \Omega, \mathbb{R}^2);\, \boldsymbol{u}_h|_K \in P_K^1(\mathbb{P}_{k+2,k}(\hat{K}, \mathbb{R}) \times \mathbb{P}_{k,k+2}(\hat{K}, \mathbb{R}))\ \forall K \in \mathcal{T}_h\}, \tag{18a}$$

$$\mathcal{P}^k_{\mathcal{ABF}} = \{p_h \in L^2(\Omega, \mathbb{R});\, p_h|_K \in P_K^0(\mathcal{R}^k_{\mathcal{ABF}}(\hat{K}))\ \forall K \in \mathcal{T}_h\}, \tag{18b}$$

where

$$\mathcal{R}^k_{\mathcal{ABF}}(\hat{K}) = \mathrm{span}\{\hat{x}_1^i \hat{x}_2^j; i, j \leq k+1, i+j < 2k+2\},$$

which is informally but incorrectly described as $\mathbb{P}_{k+1,k+1}(\hat{K}, \mathbb{R})$ without $\mathrm{span}\{\hat{x}_1^{k+1} \hat{x}_2^{k+1}\}$.

4.1. The New Spaces for Index $k \geq 0$

For each $k \geq 0$, our new spaces for planar elasticity are defined by

$$\mathbf{E}_h^k = \mathcal{S}_h^k \times \mathcal{U}_h^k \times \mathcal{R}_h^k, \tag{19}$$

with

$$\mathcal{S}_h^k = \mathcal{V}_{\mathcal{ABF}}^k \times \mathcal{V}_{\mathcal{ABF}}^k \subset H(\mathrm{div}, \Omega, \mathbb{M}), \tag{20a}$$

$$\mathcal{U}_h^k = \mathcal{P}_{\mathcal{ABF}}^k \times \mathcal{P}_{\mathcal{ABF}}^k \subset L^2(\Omega, \mathbb{R}^2), \tag{20b}$$

$$\mathcal{R}_h^k = \left\{ r \in L^2(\Omega, \mathbb{R});\, r|_K \in \mathbb{P}_k(K, \mathbb{R})\ \forall K \in \mathcal{T}_h \right\}. \tag{20c}$$

Note that $\mathcal{R}_h^k$ is unmapped.

We cannot prove stability of $\mathbf{E}_h^0$. We present two other spaces for index $k = 0$, again based on $\mathcal{ABF}_0$, but supplemented by additional functions. On the reference element $\hat{K}$, let

$$\mathbb{S}^* = \mathrm{span}\left\{ \begin{pmatrix} 0 \\ \hat{x} \end{pmatrix}, \begin{pmatrix} \hat{y} \\ 0 \end{pmatrix}, \begin{pmatrix} \hat{x}^2 \\ -2\hat{x}\hat{y} \end{pmatrix}, \begin{pmatrix} 2\hat{x}\hat{y} \\ -\hat{y}^2 \end{pmatrix}, \begin{pmatrix} \hat{x}^2\hat{y} \\ -\hat{x}\hat{y}^2 \end{pmatrix} \right\} \tag{21}$$

be a space of curl functions (so their divergences vanish) and define

$$\begin{aligned} \mathcal{V}_{\mathcal{ABF}}^{0,*}(\hat{K}) &= \mathcal{V}_{\mathcal{ABF}}^0(\hat{K}) \oplus \mathbb{S}^* \\ &= \mathbb{P}_{2,0}(\hat{K}, \mathbb{R}) \times \mathbb{P}_{0,2}(\hat{K}, \mathbb{R}) \oplus \mathbb{S}^* \subsetneq \mathbb{P}_{2,1}(\hat{K}, \mathbb{R}) \times \mathbb{P}_{1,2}(\hat{K}, \mathbb{R}). \end{aligned} \tag{22}$$

Note that the normal component is a polynomial of degree 0 for $\mathcal{V}_{\mathcal{ABF}}^0(\hat{K})$ but degree 1 for $\mathcal{V}_{\mathcal{ABF}}^{0,*}(\hat{K})$. The degrees of freedom can be defined to be the normal components and some internal degrees. The dimensions of these two spaces are 6 and 11, respectively, and they are contained in but smaller than $\mathcal{RT}_1(\hat{K}) = \mathbb{P}_{2,1}(\hat{K}, \mathbb{R}) \times \mathbb{P}_{1,2}(\hat{K}, \mathbb{R})$. The global space is

$$\mathcal{V}_{\mathcal{ABF}}^{0,*} = \{ \boldsymbol{u}_h \in H(\mathrm{div}, \Omega, \mathbb{R}^2);\, \boldsymbol{u}_h|_K \in P_K^1(\mathcal{V}_{\mathcal{ABF}}^{0,*}(\hat{K}))\ \forall K \in \mathcal{T}_h \}. \tag{23}$$

For $k = 0$, our new spaces for elasticity are defined as follows. For the stress tensor, let

$$\mathcal{S}_h^{0,*} = \mathcal{V}_{\mathcal{ABF}}^{0,*} \times \mathcal{V}_{\mathcal{ABF}}^{0,*} \subset H(\mathrm{div}, \Omega, \mathbb{M}). \tag{24}$$

For the displacement and rotation, we use (20b)–(20c). The three spaces for index $k = 0$ are then defined as $\mathbf{E}_h^0 = \mathcal{S}_h^0 \times \mathcal{U}_h^0 \times \mathcal{R}_h^0$ and

$$\mathbf{E}_h^{0,*} = \mathcal{S}_h^{0,*} \times \mathcal{U}_h^0 \times \mathcal{R}_h^0, \tag{25a}$$

$$\mathbf{E}_h^{0,*,1} = \mathcal{S}_h^{0,*} \times \mathcal{U}_h^0 \times \mathcal{R}_h^1. \tag{25b}$$

These low order spaces are all smaller than the smallest $\mathcal{RT}_1-$based spaces of Arnold et al. (2015) (although the spaces, except $\mathbf{E}_h^0$, have linear normal stresses, and so lead to a global hybridized problem of the same dimension). We can prove stability on general quadrilateral meshes only when one uses $\mathbf{E}_h^{0,*}$ and $\mathbf{E}_h^{0,*,1}$.

We remark that we have defined $\mathbb{S}^*$ in (21), but it is not clear that each of these functions is needed in general. A simple numerical experiment, reported in Section 7.2, has shown that, even in the quasi-incompressible regime, the same order of convergence and accuracy when that the last, cubic vector is not included. We call this space $\mathbb{S}^\#$:

$$\mathbb{S}^\# = \mathrm{span}\left\{ \begin{pmatrix} 0 \\ \hat{x} \end{pmatrix}, \begin{pmatrix} \hat{y} \\ 0 \end{pmatrix}, \begin{pmatrix} \hat{x}^2 \\ -2\hat{x}\hat{y} \end{pmatrix}, \begin{pmatrix} 2\hat{x}\hat{y} \\ -\hat{y}^2 \end{pmatrix} \right\}. \tag{26}$$

In this case, the global space is

$$\mathcal{V}_{\mathcal{ABF}}^{0,\#} = \{ \boldsymbol{u}_h \in H(\mathrm{div}, \Omega, \mathbb{R}^2);\, \boldsymbol{u}_h|_K \in P_K^1(\mathcal{V}_{\mathcal{ABF}}^{0,\#}(\hat{K}))\ \forall K \in \mathcal{T}_h \}, \tag{27}$$

where $\mathcal{V}^{0,\#}_{\mathcal{ABF}}(\hat{K}) = \mathcal{V}^{0}_{\mathcal{ABF}}(\hat{K}) \oplus \mathbb{S}^{\#}$. We have no proof that the resulting element would work in general.

4.2. Stability of the New Spaces

Lemma 4.1: *The spaces* $\mathbf{E}^k_h$ *for* $k \geq 1$ *and the spaces* $\mathbf{E}^{0,*}_h$ *and* $\mathbf{E}^{0,*,1}_h$ *satisfy the coercivity condition* (9) *and the inf-sup condition* (10).

Proof. The coercivity condition (9) holds for $\mathbf{E}^k_h$, $k \geq 0$, since the divergences of functions in $\mathcal{S}^k_h$ lie in $\mathcal{U}^k_h$ (Arnold et al., 2005) (one can also see this fact directly using (28)). This also holds when using $\mathcal{S}^{0,*}_h$ and $\mathcal{S}^{0,*,1}_h$, since the supplemental functions are divergence free.

We prove the inf-sup results using Lemma 3.2. The spaces $\mathcal{V}^k_{\mathcal{ABF}} \times \mathcal{P}^k_{\mathcal{ABF}}$, $k \geq 0$, are inf-sup stable for the Poisson problem, i.e., they satisfy (13) (Arnold et al., 2005). Since $\mathcal{V}^0_{\mathcal{ABF}} \subset \mathcal{V}^{0,*}_{\mathcal{ABF}}$, (13) holds for $\mathcal{V}^{0,*}_{\mathcal{ABF}} \times \mathcal{P}^0_{\mathcal{ABF}}$ as well.

We use the auxiliary spaces

$$\mathcal{W}^k_h = \left\{ \boldsymbol{w} \in H^1(\Omega, \mathbb{R}^2);\, \boldsymbol{w}|_K \in P^0_K(\mathbb{P}_{k+1,k+1}(\hat{K}, \mathbb{R}^2))\ \forall K \in \mathcal{T}_h \right\}, \quad k \geq 1,$$
$$\mathcal{W}^0_h = \mathcal{W}^1_h.$$

For each $k \geq 0$, the pair $(\mathcal{W}^k_h, \mathcal{R}^k_h)$ is Stokes-compatible, i.e., these spaces satisfy the inf-sup condition (14) (Girault & Raviart, 1986, section II.3.2). Moreover, $(\mathcal{W}^0_h, \mathcal{R}^1_h)$ is Stokes-compatible. It remains to show that $\operatorname{curl} \mathcal{W}^k_h \subset \mathcal{S}^k_h$. It is not difficult to show the relation

$$\operatorname{curl} P^0_K(\hat{v}) = P^1_K(\hat{\operatorname{curl}}\, \hat{v}), \tag{28}$$

so, on each element $K \in \mathcal{T}_h$, one has locally that for $k \geq 1$,

$$\begin{aligned}\operatorname{curl} \mathcal{W}^k_h(K) &= \operatorname{curl}(P^0_K(\mathbb{P}_{k+1,k+1}(\hat{K}, \mathbb{R}^2))) = P^1_K(\hat{\operatorname{curl}}(\mathbb{P}_{k+1,k+1}(\hat{K}, \mathbb{R}^2))) \\ &\subset \mathcal{V}^k_{\mathcal{ABF}}(K) \times \mathcal{V}^k_{\mathcal{ABF}}(K) = \mathcal{S}^k_h(K),\end{aligned}$$

and the proof is complete for $k \geq 1$. The result for $\mathbf{E}^{0,*}_h$ also holds, since $\hat{\operatorname{curl}}(\mathbb{P}_{2,2}(\hat{K}, \mathbb{R}^2)) \subset \mathcal{V}^{0,*}_{\mathcal{ABF}}(\hat{K}) \times \mathcal{V}^{0,*}_{\mathcal{ABF}}(\hat{K})$ and a similar computation shows that

$$\operatorname{curl} \mathcal{W}^0_h(K) = \operatorname{curl}(P^0_K(\mathbb{P}_{2,2}(\hat{K}, \mathbb{R}^2))) = P^1_K(\hat{\operatorname{curl}}(\mathbb{P}_{2,2}(\hat{K}, \mathbb{R}^2))) \subset \mathcal{S}^{0,*}_h(K).$$

The proof is complete. □

We conclude from Theorem 3.1 that there is a unique solution to (8) using our new spaces when $k \geq 1$ or when we use $\mathcal{S}^{0,*}_h$ or $\mathcal{S}^{0,*,1}_h$. Moreover, the stability bound (12) holds in these cases. Since trivially $\boldsymbol{I} \in \mathcal{S}^k_h$, these spaces will work well in the incompressible limit, and the inf-sup condition (11) holds.

The following result shows that the space $\mathbf{E}^0_h$ is uniformly inf-sup stable, but only on sufficiently fine meshes. In that case, Theorem 3.1 applies also to $\mathbf{E}^0_h$. We caution the reader, however, not to use $\mathbf{E}^0_h$ in the formulation (8), since the numerical results show that the meshes need to be very fine indeed to have the inf-sup condition on quadrilateral meshes.

Lemma 4.2: *If* $\partial\Omega$ *is sufficiently regular that the Stokes problem on* Ω *is regular, and if the sequence of meshes is shape regular (as defined in Section 5), then there are constants* $\beta^0_E > 0$ *and* $C^0_E > 0$ *such that*

$$\inf_{\substack{\boldsymbol{u}_h \in \mathcal{U}^0_h \\ r_h \in \mathcal{R}^0_h}} \sup_{\boldsymbol{\tau}_h \in \mathcal{S}^0_h} \frac{(\operatorname{div} \boldsymbol{\tau}_h, \boldsymbol{u}_h) + (\operatorname{asym} \boldsymbol{\tau}_h, r_h)}{\|\boldsymbol{\tau}_h\|_{\mathcal{S}} \left(\|\boldsymbol{u}_h\|_{\mathcal{U}} + \|r_h\|_{\mathcal{R}}\right)} \geq \beta^0_E - C^0_E h. \tag{29}$$

If h is sufficiantly small, then, for example, $\beta_E^0 - C_E^0 h > \frac{1}{2}\beta_E^0 > 0$.

We give the proof in the next section, since we need the operator $\boldsymbol{\pi}_0$ defined there.

5. Error Analysis

In this section we provide bounds on the difference between the exact solution and the approximate solution when using our new $\mathcal{ABF}-$based elements. We must assume that the sequence of meshes $\mathcal{T}_h$ remains shape-regular as $h \to 0$. This ensures that the mesh does not degenerate to highly elongated or nearly triangular elements. Each element $K \in \mathcal{T}_h$ contains four (overlapping) triangles constructed from any choice of three vertices, and each such triangle has an inscribed circle, the minimal radius of which is ρ_K. If h_K denotes the diameter of K, the requirement is that the ratio $\rho_K/h_K \geq \sigma_* > 0$, where σ_* is independent of $\mathcal{T}_h$. In this notation, $h = \max_{K\in\mathcal{T}_h} h_K$.

From the shape regularity, the Bramble-Hilbert (Bramble & Hilbert, 1970) or Dupont-Scott (Dupont & Scott, 1980) lemma, and the approximation results for mapped spaces in Ciarlet (1978) and Arnold et al. (2005), we conclude local consistency for any of the spaces $\mathbf{E}_h = \mathcal{S}_h \times \mathcal{U}_h \times \mathcal{R}_h$ defined in the previous section; that is, for all $\mathcal{T}_h$ and $K \in \mathcal{T}_h$, there is $C > 0$ such that

$$\inf_{\tilde{\boldsymbol{\sigma}}_h \in \mathcal{S}_h^k\big|_K} \|\boldsymbol{\sigma} - \tilde{\boldsymbol{\sigma}}_h\|_{L^2(K,\mathbb{M})} \leq C h_K^{s+1} \|\boldsymbol{\sigma}\|_{H^{s+1}(K,\mathbb{M})}\,, \qquad s = 0, 1, \ldots, k, \tag{30a}$$

$$\inf_{\tilde{\boldsymbol{\sigma}}_h \in \mathcal{S}_h^k\big|_K} \big\|\operatorname{div}(\boldsymbol{\sigma} - \tilde{\boldsymbol{\sigma}}_h)\big\|_{L^2(K,\mathbb{R}^2)} \leq C h_K^{s+1} \|\operatorname{div}\boldsymbol{\sigma}\|_{H^{s+1}(K,\mathbb{R}^2)}\,, \quad s = -1, 0, \ldots, k, \tag{30b}$$

$$\inf_{\tilde{\boldsymbol{u}}_h \in \mathcal{U}_h^k\big|_K} \|\boldsymbol{u} - \tilde{\boldsymbol{u}}_h\|_{L^2(K,\mathbb{R}^2)} \leq C h_K^{s+1} \|\boldsymbol{u}\|_{H^{s+1}(K,\mathbb{R}^2)}\,, \qquad s = -1, 0, \ldots, k, \tag{30c}$$

$$\inf_{\tilde{r}_h \in \mathcal{R}_h^k\big|_K} \|r - \tilde{r}_h\|_{L^2(K,\mathbb{R})} \leq C h_K^{s+1} \|r\|_{H^{s+1}(K,\mathbb{R})}\,, \qquad s = -1, 0, \ldots, k. \tag{30d}$$

We remark that when $k = 0$, (30a) is improved by one power ($s = 0, 1$) if the infimum is taken over $\tilde{\boldsymbol{\sigma}}_h \in \mathcal{S}_h^{0,*}\big|_K$ (Arnold et al., 2005). Moreover, (30b) and (30c) are improved by one power on meshes of parallelograms, and also on sequences of meshes that tend to parallelograms.

To achieve global consistency, we use the Raviart-Thomas or Fortin projection operator $\boldsymbol{\pi}^k_{\mathcal{ABF}}$ defined in Arnold et al. (2005). For $\boldsymbol{\varphi} \in H(\operatorname{div}, \Omega, \mathbb{R}^2) \cap L^{2+\varepsilon}(\Omega, \mathbb{R}^2)$, $\varepsilon > 0$, $\boldsymbol{\pi}^k_{\mathcal{ABF}}\boldsymbol{\varphi} \in \mathcal{V}^k_{\mathcal{ABF}}$ is constructed locally, $P_{\mathcal{P}^k_{\mathcal{ABF}}} \operatorname{div}\boldsymbol{\varphi} = \operatorname{div}(\boldsymbol{\pi}^k_{\mathcal{ABF}}\boldsymbol{\varphi})$, where $P_{\mathcal{P}^k_{\mathcal{ABF}}}$ is the L^2-orthogonal projection operator onto $\mathcal{P}^k_{\mathcal{ABF}}$, and $\boldsymbol{\pi}^k_{\mathcal{ABF}}$ is bounded in $H^1(\Omega, \mathbb{R}^2)$. We construct the tensor version of this operator, $\boldsymbol{\pi}_k$, defined for $\boldsymbol{\sigma} \in H(\operatorname{div}, \Omega, \mathbb{M}) \cap L^{2+\varepsilon}(\Omega, \mathbb{M})$, $\varepsilon > 0$, with $\boldsymbol{\pi}_k\boldsymbol{\sigma} \in \mathcal{S}_h^k$ by applying $\boldsymbol{\pi}^k_{\mathcal{ABF}}$ to each row. It satisfies the following properties:

1) $\boldsymbol{\pi}_k$ is constructed by the concatenation of locally defined operators;
2) $\boldsymbol{\pi}_k$ satisfies the commuting diagram property, i.e., $P_{\mathcal{U}_h^k} \operatorname{div}\boldsymbol{\sigma} = \operatorname{div}(\boldsymbol{\pi}_k\boldsymbol{\sigma})$, where $P_{\mathcal{U}_h^k}$ is the L^2-orthogonal projection operator onto $\mathcal{U}_h^k$;
3) $\boldsymbol{\pi}_k$ is bounded in $H^1(\Omega, \mathbb{M})$, so that (30a) and (30b) hold for $\tilde{\boldsymbol{\sigma}}_h = \boldsymbol{\pi}_k\boldsymbol{\sigma}$.

Later, we will also use the projection $P_{\mathcal{R}_h^k}$, the L^2-orthogonal projection operator onto $\mathcal{R}_h^k$.

5.1. Error Estimates for the Uniformly Stable Elements

Theorem 5.1: *Assume that the meshes are uniformly shape regular as $h \to 0$. For the $\mathcal{ABF}_k-$based elements, $\mathbf{E}_h^k$ with $k \geq 1$, $\mathbf{E}_h^{0,*}$ and $\mathbf{E}_h^{0,*,1}$, there exists a constant $C > 0$ such that*

$$\|\boldsymbol{\sigma} - \boldsymbol{\sigma}_h\|_{\mathcal{S}} + \|\boldsymbol{u} - \boldsymbol{u}_h\|_{\mathcal{U}} + \|r - r_h\|_{\mathcal{R}} \leq C h^{k+1}(\|\boldsymbol{\sigma}\|_{k+1} + \|\operatorname{div}\boldsymbol{\sigma}\|_{k+1} + \|\boldsymbol{u}\|_{k+1} + \|r\|_{k+1}), \tag{31}$$

$$\|\operatorname{div}\boldsymbol{\sigma} - \operatorname{div}\boldsymbol{\sigma}_h\|_{L^2(\Omega,\mathbb{R}^2)} \leq C h^{k+1} \|\operatorname{div}\boldsymbol{\sigma}\|_{k+1}\,. \tag{32}$$

Proof. Introducing the projections $\bar{\boldsymbol{\sigma}}_h = \boldsymbol{\pi}_k \boldsymbol{\sigma}$, $\bar{\boldsymbol{u}}_h = P_{\mathcal{U}_h^k} \boldsymbol{u}$ and $\bar{r}_h = P_{\mathcal{R}_h^k} r$ and using the triangle inequality, it suffices to show that the errors in the finite dimensional spaces $\|\bar{\boldsymbol{\sigma}}_h - \boldsymbol{\sigma}_h\|, \|\bar{\boldsymbol{u}}_h - \boldsymbol{u}_h\|$ and $\|\bar{r}_h - r_h\|$ are bounded by the projection errors $\|\boldsymbol{\sigma} - \bar{\boldsymbol{\sigma}}_h\|, \|\boldsymbol{u} - \bar{\boldsymbol{u}}_h\|$ and $\|r - \bar{r}_h\|$. By the inf-sup condition (11) there exist $(\tilde{\boldsymbol{\tau}}_h, \tilde{\boldsymbol{\eta}}_h, \tilde{s}_h) \in \mathbf{E}_h^k$ (or $\mathbf{E}_h^{0,*}$ or $\mathbf{E}_h^{0,*,1}$) such that

$$\left\|(\bar{\boldsymbol{\sigma}}_h - \boldsymbol{\sigma}_h, \bar{\boldsymbol{u}}_h - \boldsymbol{u}_h, \bar{r}_h - r_h)\right\|_E \left\|(\tilde{\boldsymbol{\tau}}_h, \tilde{\boldsymbol{\eta}}_h, \tilde{s}_h)\right\|_E \leq \gamma_E^{-1} \mathcal{A}((\bar{\boldsymbol{\sigma}}_h - \boldsymbol{\sigma}_h, \bar{\boldsymbol{u}}_h - \boldsymbol{u}_h, \bar{r}_h - r_h), (\tilde{\boldsymbol{\tau}}_h, \tilde{\boldsymbol{\eta}}_h, \tilde{s}_h)).$$

On the other hand, from (7) and (8), we have

$$\mathcal{A}((\boldsymbol{\sigma}, \boldsymbol{u}, r), (\tilde{\boldsymbol{\tau}}_h, \tilde{\boldsymbol{\eta}}_h, \tilde{s}_h)) = \mathcal{A}((\boldsymbol{\sigma}_h, \boldsymbol{u}_h, r_h), (\tilde{\boldsymbol{\tau}}_h, \tilde{\boldsymbol{\eta}}_h, \tilde{s}_h)),$$

and so

$$\begin{aligned}\mathcal{A}((\bar{\boldsymbol{\sigma}}_h - \boldsymbol{\sigma}_h, \bar{\boldsymbol{u}}_h - \boldsymbol{u}_h, \bar{r}_h - r_h), (\tilde{\boldsymbol{\tau}}_h, \tilde{\boldsymbol{\eta}}_h, \tilde{s}_h)) &= -\mathcal{A}((\boldsymbol{\sigma} - \bar{\boldsymbol{\sigma}}_h, \boldsymbol{u} - \bar{\boldsymbol{u}}_h, r - \bar{r}_h), (\tilde{\boldsymbol{\tau}}_h, \tilde{\boldsymbol{\eta}}_h, \tilde{s}_h)) \\ &\leq C\left\|(\boldsymbol{\sigma} - \bar{\boldsymbol{\sigma}}_h, \boldsymbol{u} - \bar{\boldsymbol{u}}_h, r - \bar{r}_h)\right\|_E \left\|(\tilde{\boldsymbol{\tau}}_h, \tilde{\boldsymbol{\eta}}_h, \tilde{s}_h)\right\|_E,\end{aligned}$$

which, combined with (30), shows (31).

Using that $\mathcal{U}_h^k \subset \mathcal{U}$, we can restrict (7b) to $\mathcal{U}_h^k$ and subtract from (8b):

$$(\operatorname{div} \boldsymbol{\sigma} - \operatorname{div} \boldsymbol{\sigma}_h, \boldsymbol{\eta}_h) = 0 \quad \forall \boldsymbol{\eta}_h \in \mathcal{U}_h^k.$$

By the commuting diagram property, this is

$$(\operatorname{div} \boldsymbol{\pi}_k \boldsymbol{\sigma} - \operatorname{div} \boldsymbol{\sigma}_h, \boldsymbol{\eta}_h) = 0 \quad \forall \boldsymbol{\eta}_h \in \mathcal{U}_h^k.$$

Taking $\boldsymbol{\eta}_h = \operatorname{div} \boldsymbol{\pi}_k \boldsymbol{\sigma} - \operatorname{div} \boldsymbol{\sigma}_h \in \mathcal{U}_h^k$ shows that $\operatorname{div} \boldsymbol{\pi}_k \boldsymbol{\sigma} - \operatorname{div} \boldsymbol{\sigma}_h = 0$. Finally,

$$\|\operatorname{div} \boldsymbol{\sigma} - \operatorname{div} \boldsymbol{\sigma}_h\| \leq \|\operatorname{div} \boldsymbol{\sigma} - \operatorname{div} \boldsymbol{\pi}_k \boldsymbol{\sigma}\|,$$

and the more refined result (32) follows from (30b). □

Recall that the coercivity condition (9) is independent of λ. This implies that the inf-sup condition (11) is valid even for the incompressible limit, and so are the estimates (31), i.e., the method is locking-free with respect to the incompressibility constraint.

5.2. Error Estimates for $\mathbf{E}_h^0$

Theorem 5.1 will apply to $\mathbf{E}_h^0$ for h sufficiently small once we establish Lemma 4.2. We now give its proof.

Proof (of Lemma 4.2). The proof is based on the proof of Lemma 3.2 appearing in Arnold et al. (2015). Let $\boldsymbol{u}_h \in \mathcal{U}_h$ be given. The $\mathcal{ABF}_0$ spaces are inf-sup stable for the mixed Poisson problem, so using the inf-sup condition for this problem on each component of $\boldsymbol{u}_h$, we deduce that there exists a tensor $\bar{\boldsymbol{\tau}}_h \in \mathcal{S}_h$ such that

$$(\operatorname{div} \bar{\boldsymbol{\tau}}_h, \boldsymbol{u}_h) = \|\boldsymbol{u}_h\|_{\mathcal{U}}^2 \quad \text{and} \quad \|\bar{\boldsymbol{\tau}}_h\|_{\mathcal{S}} \leq \beta_P^{-1} \|\boldsymbol{u}_h\|_{\mathcal{U}}.$$

Now for $r_h \in \mathcal{R}_h^0$ we solve for $(\boldsymbol{w}, \phi)$ the Stokes problem on Ω,

$$\begin{aligned}-\Delta \boldsymbol{w} + \nabla \phi &= \mathbf{0}, \\ \operatorname{div} \boldsymbol{w} &= r_h - P_{\mathcal{R}_h^0} \operatorname{asym} \bar{\boldsymbol{\tau}}_h.\end{aligned}$$

By the regularity hypothesis,

$$\|\boldsymbol{w}\|_{H^2(\Omega)} \leq C\|r_h - P_{\mathcal{R}_h^0}\operatorname{asym}\bar{\boldsymbol{\tau}}_h\|.$$

Let $\bar{\bar{\boldsymbol{\tau}}}_h = -\boldsymbol{\pi}_0 \operatorname{curl}\boldsymbol{w} \in \mathcal{S}_h^0$ (the curl operator is applied to each row of $\boldsymbol{w}$), and let $\tilde{\boldsymbol{\tau}}_h = \bar{\boldsymbol{\tau}}_h + \bar{\bar{\boldsymbol{\tau}}}_h$.

Note that $P_{\mathcal{U}_h^0}\operatorname{div}\bar{\bar{\boldsymbol{\tau}}}_h = \boldsymbol{0}$ by the commuting diagram property and that $\operatorname{div}\boldsymbol{w} = -\operatorname{asym}(\operatorname{curl}\boldsymbol{w})$. We compute, for some constants $C_i > 0$, $i = 1, 2, 3$,

$$\begin{aligned}
&(\operatorname{div}\tilde{\boldsymbol{\tau}}_h, \boldsymbol{u}_h) + (\operatorname{asym}\tilde{\boldsymbol{\tau}}_h, r_h)\\
&\quad= (\operatorname{div}\bar{\boldsymbol{\tau}}_h, \boldsymbol{u}_h) + (\operatorname{asym}\bar{\boldsymbol{\tau}}_h, r_h) - (\operatorname{asym}(\boldsymbol{\pi}_0\operatorname{curl}\boldsymbol{w}), r_h)\\
&\quad= \|\boldsymbol{u}_h\|_{\mathcal{U}}^2 + (\operatorname{asym}\bar{\boldsymbol{\tau}}_h, r_h) - (\operatorname{asym}(\operatorname{curl}\boldsymbol{w}), r_h) - (\operatorname{asym}((\boldsymbol{\pi}_0 - \boldsymbol{I})\operatorname{curl}\boldsymbol{w}), r_h)\\
&\quad= \|\boldsymbol{u}_h\|_{\mathcal{U}}^2 + \|r_h\|_{\mathcal{R}}^2 - (\operatorname{asym}((\boldsymbol{\pi}_0 - \boldsymbol{I})\operatorname{curl}\boldsymbol{w}), r_h)\\
&\quad\geq \|\boldsymbol{u}_h\|_{\mathcal{U}}^2 + \|r_h\|_{\mathcal{R}}^2 - C_1\|(\boldsymbol{\pi}_0 - \boldsymbol{I})\operatorname{curl}\boldsymbol{w}\|_{L^2}\,\|r_h\|_{\mathcal{R}}\\
&\quad\geq \|\boldsymbol{u}_h\|_{\mathcal{U}}^2 + \|r_h\|_{\mathcal{R}}^2 - C_2\|\boldsymbol{w}\|_{H^2}\,h\,\|r_h\|_{\mathcal{R}}\\
&\quad\geq \|\boldsymbol{u}_h\|_{\mathcal{U}}^2 + \|r_h\|_{\mathcal{R}}^2 - C_3\big(\|\boldsymbol{u}_h\|_{\mathcal{U}} + \|r_h\|_{\mathcal{R}}\big)\|r_h\|_{\mathcal{R}}\,h,
\end{aligned}$$

using the approximation property of $\boldsymbol{\pi}_0$. Then, for some constant $C_4 > 0$,

$$\begin{aligned}
\sup_{\boldsymbol{\tau}_h\in\mathcal{S}_h}\frac{(\operatorname{div}\boldsymbol{\tau}_h, \boldsymbol{u}_h) + (\operatorname{asym}\boldsymbol{\tau}_h, r_h)}{\|\boldsymbol{\tau}_h\|_{\mathcal{S}}} &\geq \frac{(\operatorname{div}\tilde{\boldsymbol{\tau}}_h, \boldsymbol{u}_h) + (\operatorname{asym}\tilde{\boldsymbol{\tau}}_h, r_h)}{\|\tilde{\boldsymbol{\tau}}_h\|_{\mathcal{S}}}\\
&\geq \frac{\|\boldsymbol{u}_h\|_{\mathcal{U}}^2 + \|r_h\|_{\mathcal{R}}^2 - C_3\big(\|\boldsymbol{u}_h\|_{\mathcal{U}} + \|r_h\|_{\mathcal{R}}\big)\|r_h\|_{\mathcal{R}}\,h}{C_4\big(\|\boldsymbol{u}_h\|_{\mathcal{U}} + \|r_h\|_{\mathcal{R}}\big)}\\
&\geq \frac{1}{2C_4}\big(\|\boldsymbol{u}_h\|_{\mathcal{U}} + \|r_h\|_{\mathcal{R}}\big) - \frac{C_3}{C_4}\|r_h\|_{\mathcal{R}}\,h,
\end{aligned}$$

and the proof is complete. □

Numerical results suggest that the variable r_h is not uniformly stable, but exhibits a checkerboard instability on quadrilateral meshes that pollutes the results unless h is small enough. That is, the asymmetries of the discrete tensors do not control r_h in the one term $(r_h, \operatorname{asym}\boldsymbol{\tau}_h)$ of (8) in which it appears within. It is natural to ask if the inclusion of a type of local bubble function into $\mathcal{S}_h^0$ would stabilize the rotations independently of the displacements. That is, we want a function $\boldsymbol{B}$ defined to be zero on Ω except on an element $K \in \mathcal{T}_h$, and such that $\operatorname{div}\boldsymbol{B} = 0$ and $\boldsymbol{B}\cdot\boldsymbol{\nu} = 0$ on ∂K. Include the span of this function in the rows of each tensor of $\mathcal{S}_h^0(K)$. Then if the average asymmetry of these bubble tensors does not vanish, we can construct a $\boldsymbol{\tau}_h$ with vanishing divergence and any prescribed $\operatorname{asym}\boldsymbol{\tau}_h$. However, all such bubbles have components with vanishing average. To see this, simply compute

$$(B_i, 1)_K = (\boldsymbol{B}, e_i)_K = (\boldsymbol{B}, \nabla x_i)_K = (\operatorname{div}\boldsymbol{B}, x_i)_K = 0.$$

We conclude that no local stabilization method can improve the formulation (8). Perhaps some stabilization strategy can be designed for $\mathbf{E}_h^0$, but this is beyond the scope of the present paper. If we add instead a non-divergence-free function, we must increase the order of the tractions on the edges of the elements, $\boldsymbol{\tau}_h\boldsymbol{\nu}$, to higher order polynomials than constants. This leads us to $\mathbf{E}_h^{0,*}$, $\mathbf{E}_h^{0,*,1}$ and even $\mathbf{E}_h^{0,\#}$.

5.3. Improved Error Estimates for $\mathbf{E}_h^{0,*,1}$

We observe rates of convergence (see Section 7) improved from those guaranteed by Theorem 5.1 when $\mathbf{E}_h^{0,*,1}$ is used. Here we prove that these improved rates are to be expected.

Below, we introduce the projection $\hat{\boldsymbol{\pi}}_{\mathcal{ABF}}^{0,*}\hat{\boldsymbol{u}} \in \mathcal{V}_{\mathcal{ABF}}^{0,*}(\hat{K})$, for $\hat{\boldsymbol{u}} \in H(\operatorname{div}, \hat{K}, \mathbb{R}^2) \cap L^{2+\varepsilon}(\hat{K}, \mathbb{R}^2)$, $\varepsilon > 0$. For $\boldsymbol{u} \in H(\operatorname{div}, \Omega, \mathbb{R}^2) \cap L^{2+\varepsilon}(\Omega, \mathbb{R}^2), \varepsilon > 0$, we can then define the projection $\boldsymbol{\pi}_{\mathcal{ABF}}^{0,*}\boldsymbol{u} \in \mathcal{V}_{\mathcal{ABF}}^{0,*}$ locally from $\hat{\boldsymbol{\pi}}_{\mathcal{ABF}}^{0,*}$ using

the Piola mapping, $\boldsymbol{\pi}^{0,*}_{\mathcal{ABF}}\Big|_K = P^1_K \circ \hat{\boldsymbol{\pi}}^{0,*}_{\mathcal{ABF}} \circ (P^1_K)^{-1}$, and requiring that the edge degrees of freedom coincide on every internal edge in $\mathcal{T}_h$. Finally, a projection operator $\boldsymbol{\pi}^{0,*}$ is defined for $\boldsymbol{\sigma} \in H(\mathrm{div}, \Omega, \mathbb{M}) \cap L^{2+\varepsilon}(\Omega, \mathbb{M})$, $\varepsilon > 0$, with $\boldsymbol{\pi}^{0,*}\boldsymbol{\sigma} \in \mathcal{S}^{0,*}_h$, by applying $\boldsymbol{\pi}^{0,*}_{\mathcal{ABF}}$ to each row.

The following degrees of freedom are taken for $\hat{\boldsymbol{\pi}}^{0,*}_{\mathcal{ABF}}$ on the reference element $\hat{K} = [-1,1]^2$:

$$\langle \hat{\boldsymbol{u}} \cdot \hat{\boldsymbol{\nu}}, 1 \rangle_{\hat{e}}, \qquad \text{for each edge } \hat{e} \text{ of } \hat{K}, \tag{33a}$$

$$(\hat{\mathrm{div}}\hat{\boldsymbol{u}}, \hat{q})_{\hat{K}}, \qquad \hat{q} \in \{\hat{x}, \hat{y}\}, \tag{33b}$$

$$\langle \hat{u}_2, \hat{x} \rangle_{\hat{e}_\pm}, \qquad \text{on } \hat{e}_\pm = \{-1 < \hat{x} < 1, \hat{y} = \pm 1\} \tag{33c}$$

$$\langle \hat{u}_1, \hat{y} \rangle_{\hat{e}_\pm}, \qquad \text{on } \hat{e}_\pm = \{\hat{x} = \pm 1, -1 < \hat{y} < 1\}, \tag{33d}$$

$$(\hat{u}_1\hat{y} - \hat{u}_2\hat{x}, 1)_{\hat{K}}. \tag{33e}$$

Lemma 5.2: *The degrees of freedom for $\hat{\boldsymbol{\pi}}^{0,*}_{\mathcal{ABF}}$ are unisolvent for any function $\hat{\boldsymbol{u}} \in \mathcal{V}^{0,*}_{\mathcal{ABF}}(\hat{K})$. Moreover, the restriction of $\hat{\boldsymbol{u}} \cdot \hat{\boldsymbol{\nu}}$ to any edge is uniquely defined by the degrees of freedom on that edge. This ensures that the assembled basis functions will be in $H(\mathrm{div}, \Omega, \mathbb{R}^2)$.*

Proof. Let $\hat{\boldsymbol{u}} \in \mathcal{V}^{0,*}_{\mathcal{ABF}}(\hat{K})$. Then

$$\hat{\boldsymbol{u}} = \hat{\boldsymbol{u}}_{\mathcal{ABF}_0} + a\begin{pmatrix}0\\ \hat{x}\end{pmatrix} + b\begin{pmatrix}\hat{y}\\ 0\end{pmatrix} + c\begin{pmatrix}\hat{x}^2 - 1\\ -2\hat{x}\hat{y}\end{pmatrix} + d\begin{pmatrix}-2\hat{x}\hat{y}\\ \hat{y}^2 - 1\end{pmatrix} + e\begin{pmatrix}\hat{x}^2\hat{y}\\ -\hat{x}\hat{y}^2\end{pmatrix},$$

with $\hat{\boldsymbol{u}}_{\mathcal{ABF}_0} \in \mathcal{V}^0_{\mathcal{ABF}}(\hat{K})$. Suppose the degrees of freedom (33) vanish. The degrees of freedom (33c)–(33e) for $\hat{\boldsymbol{u}}_{\mathcal{ABF}_0}$ vanish by orthogonality of $\hat{x}$ and $\hat{y}$ to 1 on $[-1,1]$. From (33c) we get $a - e \mp 2c = 0$, which implies $c = 0$ and $a = e$. From (33d) we get similarly $b + e \mp 2d = 0$, which implies $d = 0$ and $b = -e$. Using (33e) we get $3b - 3a + 2e = 0$, which implies $a = b = e = 0$; therefore, $\hat{\boldsymbol{u}} = \hat{\boldsymbol{u}}_{\mathcal{ABF}_0} \in \mathcal{V}^0_{\mathcal{ABF}}(\hat{K})$. Since (33a) and (33b) are unisolvent degrees of freedom for $\mathcal{V}^0_{\mathcal{ABF}}(\hat{K})$ (Arnold et al., 2005, Sec. 4), it follows that $\hat{\boldsymbol{u}} = \boldsymbol{0}$ and the degrees of freedom (33) are unisolvent.

From (33a) and (33c)–(33d), note that if the degrees of freedom on an edge $\hat{e}$ vanish, then $\hat{\boldsymbol{u}} \cdot \hat{\boldsymbol{\nu}}$ vanishes on $\hat{e}$, since $\hat{\boldsymbol{u}} \cdot \hat{\boldsymbol{\nu}} \in \mathbb{P}_1(\hat{e})$ on any edge $\hat{e}$ of $\hat{K}$. □

Lemma 5.3: *For all $\mathcal{T}_h$ and $K \in \mathcal{T}_h$ a convex quadrilateral, there is a $C > 0$ such that*

$$\left\| \boldsymbol{\sigma} - \boldsymbol{\pi}^{0,*}\boldsymbol{\sigma} \right\|_{L^2(K,\mathbb{M})} \leq C h_K^2 |\boldsymbol{\sigma}|_{H^2(K,\mathbb{M})} \quad \forall \boldsymbol{\sigma} \in H^2(K, \mathbb{M}).$$

Proof. The result follows from the shape regularity of K and from (Arnold et al., 2005, Theorem 4.1), noting that on the reference element $\mathcal{V}^{0,*}_{\mathcal{ABF}}(\hat{K}) = \mathcal{S}_1$, where $\mathcal{S}_1$ is the smallest space capable of furnishing $\mathcal{O}(h^2)$ approximation in the L^2-norm on arbitrary convex quadrilaterals after being submitted to the Piola transform. □

Theorem 5.4: *Assume that the meshes are uniformly shape regular as $h \to 0$. For $\mathbf{E}^{0,*,1}_h$,*

$$\|\boldsymbol{\sigma} - \boldsymbol{\sigma}_h\|_{L^2} + \|r - r_h\|_{L^2} \leq C h^2 (\|\boldsymbol{\sigma}\|_2 + \|r\|_2). \tag{34}$$

Proof. This result follows from the improved estimates by (Juntunen & Lee, 2014, Theorem 4.1) or (Lee, 2016, Theorem 2), Lemma 5.3 and (30d). □

6. Hybrid Formulation of the Elasticity Problem

The set of all edges in $\mathcal{T}_h$ is denoted by $\mathcal{E}_h$ and $\mathcal{E}_h^\Gamma$ is the set of all edges on $\Gamma = \partial\Omega$. Let $\mathcal{E}_h^0 = \mathcal{E}_h \setminus \mathcal{E}_h^\Gamma$ denote the set of interior edges in $\mathcal{T}_h$. The construction of finite dimensional spaces in $H(\mathrm{div}, \Omega, \mathbb{M})$ traditionally resembles that of subspaces of $H(\mathrm{div}, \Omega, \mathbb{R}^2)$. First, a finite dimensional space $\hat{\mathcal{S}}_h$ (usually based on polynomials) is defined on a reference element $\hat{K}$; then an approximation space $\mathcal{S}$ is built by the application of the Piola mapping to $\hat{\mathcal{S}}_h$ in each element $K \in \mathcal{T}_h$. The degrees of freedom are chosen in such a way that $\mathcal{S} \subset H(\mathrm{div}, \Omega, \mathbb{M})$, i.e., that the approximated traction is uniquely defined on each edge of $\mathcal{E}_h^0$. This last step can by simplified by the introduction of a Lagrange multiplier and by the addition of an equation that allows for the continuity of the traction to be imposed via a variational formulation. The Lagrange multiplier is defined in the space

$$\mathcal{L}_h^{\boldsymbol{\varphi}} := \{\, \hat{\boldsymbol{u}}|_e \in \mathbb{P}_k(e, \mathbb{R}^2)\ \forall e \in \mathcal{E}_h;\ \hat{\boldsymbol{u}}|_e = P_{\mathbb{P}_k(e,\mathbb{R}^2)}\, \boldsymbol{\varphi}|_e\ \forall e \in \mathcal{E}_h^\Gamma\}, \tag{35}$$

where $P_{\mathbb{P}_k(e,\mathbb{R}^2)}$ is the local L^2-projection onto $\mathbb{P}_k(e, \mathbb{R}^2)$, and the approximation for the stress field is sought in the larger, less restrictive space

$$\bar{\mathcal{S}}_h := \{\boldsymbol{\sigma} \in L^2(\Omega, \mathbb{M});\ \mathrm{div}\, \boldsymbol{\sigma}|_K \in \mathcal{S}_h(K)\ \forall K \in \mathcal{T}_h\},$$

which is $\mathcal{S}_h$ locally but without the constraint that the space lies in $H(\mathrm{div}, \Omega, \mathbb{M})$, i.e., the normal continuity constraint on the edges of the elements is relaxed.

We then introduce a mixed hybrid formulation of the elasticity problem, which is equivalent to the Discrete Elasticity Problem (8), as follows.

Hybrid Formulation of the Elasticity Problem: *Given* $\boldsymbol{u}_\mathrm{B} \in H^{1/2}(\Gamma, \mathbb{R}^2)$ *and* $\boldsymbol{g} \in L^2(\Omega, \mathbb{R}^2)$*, find* $(\boldsymbol{\sigma}_h, \boldsymbol{u}_h, r_h, \hat{\boldsymbol{u}}_h) \in \bar{\mathcal{S}}_h \times \mathcal{U}_h \times \mathcal{R}_h \times \mathcal{L}_h^{\boldsymbol{u}_\mathrm{B}}$ *such that*

$$\sum_{K\in\mathcal{T}_h} \Big[(\boldsymbol{A}\boldsymbol{\sigma}_h, \boldsymbol{\tau})_K + (\boldsymbol{u}_h, \mathrm{div}\, \boldsymbol{\tau})_K + (r_h, \mathrm{asym}\, \boldsymbol{\tau})_K - \langle \hat{\boldsymbol{u}}_h, \boldsymbol{\tau}\boldsymbol{\nu}\rangle_{\partial K \cap \mathcal{E}_h^0}\Big] = 0 \quad \forall \boldsymbol{\tau} \in \bar{\mathcal{S}}_h, \tag{36a}$$

$$\sum_{K\in\mathcal{T}_h} (\mathrm{div}\, \boldsymbol{\sigma}_h, \boldsymbol{\eta})_K = (\boldsymbol{g}, \boldsymbol{\eta}) \qquad \forall \boldsymbol{\eta} \in \mathcal{U}_h, \tag{36b}$$

$$\sum_{K\in\mathcal{T}_h} (\mathrm{asym}\, \boldsymbol{\sigma}_h, s)_K = 0 \qquad \forall s \in \mathcal{R}_h, \tag{36c}$$

$$\sum_{K\in\mathcal{T}_h} \langle \boldsymbol{\sigma}_h\boldsymbol{\nu}, \hat{\boldsymbol{\eta}}\rangle_{\partial K \cap \mathcal{E}_h^0} = 0 \qquad \forall \hat{\boldsymbol{\eta}} \in \mathcal{L}_h^{\boldsymbol{0}}. \tag{36d}$$

The hybrid formulation shall be used in the actual implementation, aiming to facilitate the construction of local restrictions of the finite dimensional spaces and, through a static condensation technique, to reduce the number of degrees of freedom in the global problem only to those corresponding to the Lagrange multiplier $\hat{\boldsymbol{u}}_h$. Also, the resulting algebraic system of equations for the Lagrange multiplier is positive-definite. The remaining variables are the solution, on each element $K \in \mathcal{T}_h$, of the mixed formulation for elasticity with weakly imposed symmetry (8): *Given* $\hat{\boldsymbol{u}}_h \in \mathcal{L}_h^{\boldsymbol{u}_\mathrm{B}}$ *and* $\boldsymbol{g} \in L^2(\Omega, \mathbb{R}^2)$*, find* $(\boldsymbol{\sigma}_h, \boldsymbol{u}_h, r_h) \in \bar{\mathcal{S}}_h \times \mathcal{U}_h \times \mathcal{R}_h$ *such that, for each* $K \in \mathcal{T}_h$*,*

$$(\boldsymbol{A}\boldsymbol{\sigma}_h, \boldsymbol{\tau})_K + (\boldsymbol{u}_h, \mathrm{div}\, \boldsymbol{\tau})_K + (r_h, \mathrm{asym}\, \boldsymbol{\tau})_K = \langle \hat{\boldsymbol{u}}_h, \boldsymbol{\tau}\boldsymbol{\nu}\rangle_{\partial K} \quad \forall \boldsymbol{\tau} \in \bar{\mathcal{S}}_h, \tag{37a}$$

$$(\mathrm{div}\, \boldsymbol{\sigma}_h, \boldsymbol{\eta})_K = (\boldsymbol{g}, \boldsymbol{\eta})_K \qquad \forall \boldsymbol{\eta} \in \mathcal{U}_h, \tag{37b}$$

$$(\mathrm{asym}\, \boldsymbol{\sigma}_h, s)_K = 0 \qquad \forall s \in \mathcal{R}_h. \tag{37c}$$

The incompressible case can be handled in this formulation, as long as one avoids the loss of coercivity in (9) due to the globally constant mode in $\mathrm{tr}\, \boldsymbol{\sigma}$. In our implementation, however, we simply keep λ finite and approximate the incompressible case with a very large value for λ. Then, the local problems (37) can be solved uniquely without

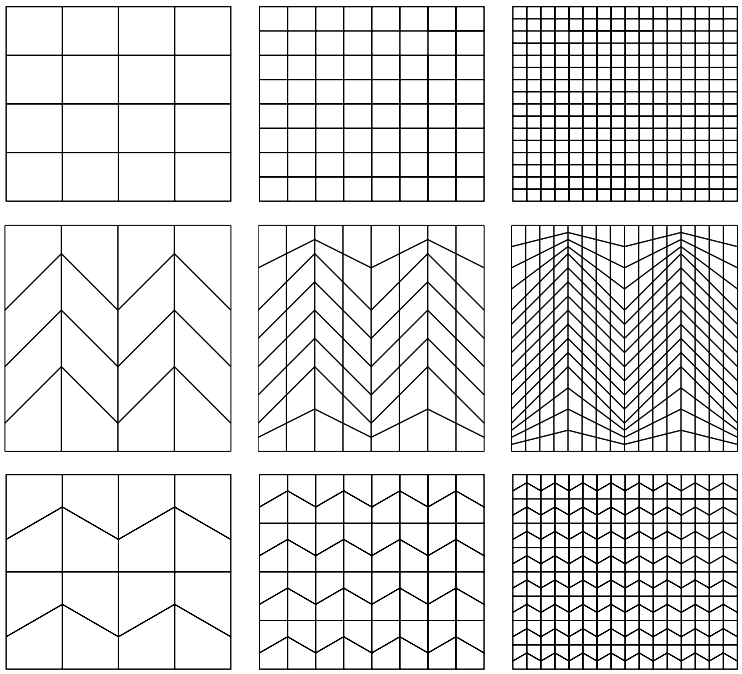

Figure 1: Sequences of meshes: square (top), asymptotically parallelogram (center row), and trapezoidal (bottom) with $n = 4$ (left), $n = 8$ (center column), and $n = 16$ (right).

the additional consideration on the trace of $\boldsymbol{\sigma}$.

7. Numerical Experiments

In this section we present convergence studies for the proposed $\mathcal{ABF}-$based spaces for linear elasticity and the corresponding $\mathcal{RT}-$based spaces of Arnold et al. (2015). Two test problems are considered: the first one is based on the compressible test presented in Arnold et al. (2015) and the second one is introduced in order to check the behavior of the full-$H(\mathrm{div})$ families, within the weakly imposed symmetry mixed formulation, on the quasi-incompressible regime. In both tests the domain is the unit square $\Omega = (0,1) \times (0,1)$, with a Dirichlet boundary condition on Γ. Three sequences of meshes are used for the numerical experiments (see Figure 1): the first one is a uniform mesh of n^2 square elements; the second mesh is constructed by the regular subdivision of an initial mesh with 8 trapezoids of base h and parallel vertical edges of size $h/2$ and $3h/2$ and 8 parallelograms of vertical edges of size h, resulting in an asymptotically parallelogram sequence; the last mesh consists of n^2 trapezoids of base h and parallel vertical edges of size $2h/3$ and $4h/3$, as proposed by Arnold et al. (2002).

7.1. Compressible Case

This first experiment compares the approximation spaces suggested by Arnold et al. (2015) (indicated by $\mathcal{RT}_1$) to the $\mathbf{E}_h^1$ spaces introduced in Section 4. As the test problem we take the analytical solution for displacement

$$\boldsymbol{u}(x_1, x_2) = \begin{bmatrix} \cos(\pi x_1)\sin(2\pi x_2) \\ \sin(\pi x_1)\cos(\pi x_2) \end{bmatrix}.$$

The body force $\boldsymbol{g}$ is computed from the exact solution and the Lamé parameters $\lambda = 123$ and $\mu = 79.3$.

Approximation errors and convergence rates in the L^2 norm for $\boldsymbol{\sigma}$, $\mathrm{div}(\boldsymbol{\sigma})$, $\boldsymbol{u}$ and r on a sequence of meshes of squares are shown in Table 1. As expected, on this affine mesh there is no difficulty in obtaining approximations

Table 1: Convergence results on meshes of squares – compressible regime.

n	$\|\boldsymbol{\sigma}-\boldsymbol{\sigma}_h\|$ error	order	$\|\mathrm{div}(\boldsymbol{\sigma}-\boldsymbol{\sigma}_h)\|$ error	order	$\|\boldsymbol{u}-\boldsymbol{u}_h\|$ error	order	$\|r-r_h\|$ error	order
$\mathcal{RT}_1-$based								
32	$7.640\cdot10^{-1}$	2.01	$5.380\cdot10^{0}$	2.00	$7.825\cdot10^{-4}$	2.00	$3.513\cdot10^{-3}$	2.00
64	$1.905\cdot10^{-1}$	2.00	$1.345\cdot10^{0}$	2.00	$1.957\cdot10^{-4}$	2.00	$8.781\cdot10^{-4}$	2.00
128	$4.759\cdot10^{-2}$	2.00	$3.364\cdot10^{-1}$	2.00	$4.893\cdot10^{-5}$	2.00	$2.195\cdot10^{-4}$	2.00
256	$1.189\cdot10^{-2}$	2.00	$8.410\cdot10^{-2}$	2.00	$1.223\cdot10^{-5}$	2.00	$5.488\cdot10^{-5}$	2.00
512	$2.973\cdot10^{-3}$	2.00	$2.103\cdot10^{-2}$	2.00	$3.058\cdot10^{-6}$	2.00	$1.372\cdot10^{-5}$	2.00
$\mathbf{E}_h^1$								
32	$7.640\cdot10^{-1}$	2.01	$8.610\cdot10^{-2}$	3.00	$2.196\cdot10^{-5}$	2.99	$3.513\cdot10^{-3}$	2.00
64	$1.905\cdot10^{-1}$	2.00	$1.076\cdot10^{-2}$	3.00	$2.751\cdot10^{-6}$	3.00	$8.781\cdot10^{-4}$	2.00
128	$4.759\cdot10^{-2}$	2.00	$1.346\cdot10^{-3}$	3.00	$3.442\cdot10^{-7}$	3.00	$2.195\cdot10^{-4}$	2.00
256	$1.189\cdot10^{-2}$	2.00	$1.682\cdot10^{-4}$	3.00	$4.304\cdot10^{-8}$	3.00	$5.488\cdot10^{-5}$	2.00
512	$2.973\cdot10^{-3}$	2.00	$2.103\cdot10^{-5}$	3.00	$5.381\cdot10^{-9}$	3.00	$1.372\cdot10^{-5}$	2.00

with convergence rate $\mathcal{O}(h^2)$: the finite dimensional spaces introduced by Arnold et al. (2015) satisfy the minimal requirements for approximation with optimal order (Arnold et al., 2005). When the new $\mathcal{ABF}_1-$based element introduced in Section 4 is used we observe one order higher convergence for $\|\mathrm{div}\,\boldsymbol{\sigma}-\mathrm{div}\,\boldsymbol{\sigma}_h\|$ and $\|\boldsymbol{u}-\boldsymbol{u}_h\|$, as expected from the polynomial approximation theory. The same comments can be made for the convergence rates on asymptotically parallelogram meshes, shown in Table 2.

The results for the sequence of trapezoidal meshes are presented in Table 3. In this case the $\mathcal{RT}_1-$based element is not capable of providing approximations for $\|\mathrm{div}\,\boldsymbol{\sigma}-\mathrm{div}\,\boldsymbol{\sigma}_h\|$ with convergence rate $\mathcal{O}(h^2)$, which is in accordance with the theory. The $\mathbf{E}_h^1$ element, however, satisfies the necessary conditions for optimal order approximation on arbitrary convex quadrilaterals.

Next we verify the convergence rates for the lowest order spaces introduced in Section 4.1: the $\mathbf{E}_h^0$ space, stable for h sufficiently small, and the enriched spaces $\mathbf{E}_h^{0,*}$ and $\mathbf{E}_h^{0,*,1}$. For brevity we only show results for meshes of asymptotically parallelogram (Table 4) and trapezoidal (Table 5) elements; the behavior of these spaces on square meshes is similar to that shown in Table 4. Comparing $\mathbf{E}_h^{0,*}$ and $\mathbf{E}_h^{0,*,1}$ we confirm that using $\mathcal{R}_h^1$ instead of $\mathcal{R}_h^0$ to approximate the rotation allows for $\mathcal{O}(h^2)$ convergence in the L^2-norm of not just the error in the rotation, but also in the stress approximation, which is in accordance with the coupled error estimate shown by Stenberg (1988) and used in Theorem 5.4.

Table 2: Convergence results on meshes of asymptotically parallelogram elements – compressible regime.

	$\|\boldsymbol{\sigma}-\boldsymbol{\sigma}_h\|$		$\left\|\operatorname{div}(\boldsymbol{\sigma}-\boldsymbol{\sigma}_h)\right\|$		$\|\boldsymbol{u}-\boldsymbol{u}_h\|$		$\|r-r_h\|$	
n	error	order	error	order	error	order	error	order
$\mathcal{RT}_1-$based								
32	$1.265\cdot10^{0}$	2.03	$1.010\cdot10^{1}$	2.00	$1.389\cdot10^{-3}$	2.00	$6.230\cdot10^{-3}$	2.00
64	$3.131\cdot10^{-1}$	2.01	$2.526\cdot10^{0}$	2.00	$3.473\cdot10^{-4}$	2.00	$1.555\cdot10^{-3}$	2.00
128	$7.795\cdot10^{-2}$	2.01	$6.315\cdot10^{-1}$	2.00	$8.684\cdot10^{-5}$	2.00	$3.883\cdot10^{-4}$	2.00
256	$1.945\cdot10^{-2}$	2.00	$1.579\cdot10^{-1}$	2.00	$2.171\cdot10^{-5}$	2.00	$9.702\cdot10^{-5}$	2.00
512	$4.858\cdot10^{-3}$	2.00	$3.947\cdot10^{-2}$	2.00	$5.427\cdot10^{-6}$	2.00	$2.425\cdot10^{-5}$	2.00
$\mathbf{E}_h^1$								
32	$1.264\cdot10^{0}$	2.03	$2.300\cdot10^{-1}$	3.01	$5.220\cdot10^{-5}$	2.98	$6.228\cdot10^{-3}$	2.00
64	$3.131\cdot10^{-1}$	2.01	$2.868\cdot10^{-2}$	3.00	$6.581\cdot10^{-6}$	2.99	$1.555\cdot10^{-3}$	2.00
128	$7.795\cdot10^{-2}$	2.01	$3.582\cdot10^{-3}$	3.00	$8.263\cdot10^{-7}$	2.99	$3.883\cdot10^{-4}$	2.00
256	$1.945\cdot10^{-2}$	2.00	$4.477\cdot10^{-4}$	3.00	$1.035\cdot10^{-7}$	3.00	$9.702\cdot10^{-5}$	2.00
512	$4.858\cdot10^{-3}$	2.00	$5.596\cdot10^{-5}$	3.00	$1.296\cdot10^{-8}$	3.00	$2.425\cdot10^{-5}$	2.00

Table 3: Convergence results on meshes of trapezoids – compressible regime.

	$\|\boldsymbol{\sigma}-\boldsymbol{\sigma}_h\|$		$\left\|\operatorname{div}(\boldsymbol{\sigma}-\boldsymbol{\sigma}_h)\right\|$		$\|\boldsymbol{u}-\boldsymbol{u}_h\|$		$\|r-r_h\|$	
n	error	order	error	order	error	order	error	order
$\mathcal{RT}_1-$based								
32	$1.026\cdot10^{0}$	2.00	$2.607\cdot10^{1}$	1.13	$9.931\cdot10^{-4}$	2.00	$4.560\cdot10^{-3}$	2.00
64	$2.563\cdot10^{-1}$	2.00	$1.270\cdot10^{1}$	1.04	$2.484\cdot10^{-4}$	2.00	$1.139\cdot10^{-3}$	2.00
128	$6.405\cdot10^{-2}$	2.00	$6.310\cdot10^{0}$	1.01	$6.209\cdot10^{-5}$	2.00	$2.847\cdot10^{-4}$	2.00
256	$1.601\cdot10^{-2}$	2.00	$3.149\cdot10^{0}$	1.00	$1.552\cdot10^{-5}$	2.00	$7.118\cdot10^{-5}$	2.00
512	$4.002\cdot10^{-3}$	2.00	$1.574\cdot10^{0}$	1.00	$3.881\cdot10^{-6}$	2.00	$1.779\cdot10^{-5}$	2.00
$\mathbf{E}_h^1$								
32	$1.035\cdot10^{0}$	2.00	$7.652\cdot10^{-1}$	2.07	$4.604\cdot10^{-5}$	2.81	$4.598\cdot10^{-3}$	2.00
64	$2.586\cdot10^{-1}$	2.00	$1.889\cdot10^{-1}$	2.02	$7.841\cdot10^{-6}$	2.55	$1.150\cdot10^{-3}$	2.00
128	$6.465\cdot10^{-2}$	2.00	$4.707\cdot10^{-2}$	2.00	$1.651\cdot10^{-6}$	2.25	$2.874\cdot10^{-4}$	2.00
256	$1.616\cdot10^{-2}$	2.00	$1.176\cdot10^{-2}$	2.00	$3.908\cdot10^{-7}$	2.08	$7.185\cdot10^{-5}$	2.00
512	$4.040\cdot10^{-3}$	2.00	$2.939\cdot10^{-3}$	2.00	$9.630\cdot10^{-8}$	2.02	$1.796\cdot10^{-5}$	2.00

Table 4: Convergence results for the lowest order spaces on meshes of asymptotically parallelogram elements – compressible regime.

	$\|\boldsymbol{\sigma}-\boldsymbol{\sigma}_h\|$		$\|\mathrm{div}(\boldsymbol{\sigma}-\boldsymbol{\sigma}_h)\|$		$\|\boldsymbol{u}-\boldsymbol{u}_h\|$		$\|r-r_h\|$	
n	error	order	error	order	error	order	error	order
				$\mathbf{E}_h^0$				
32	$4.332 \cdot 10^{1}$	1.00	$1.848 \cdot 10^{1}$	1.99	$2.874 \cdot 10^{-3}$	1.99	$1.378 \cdot 10^{-1}$	1.01
64	$2.167 \cdot 10^{1}$	1.00	$4.631 \cdot 10^{0}$	2.00	$7.197 \cdot 10^{-4}$	2.00	$6.875 \cdot 10^{-2}$	1.00
128	$1.083 \cdot 10^{1}$	1.00	$1.158 \cdot 10^{0}$	2.00	$1.800 \cdot 10^{-4}$	2.00	$3.435 \cdot 10^{-2}$	1.00
256	$5.417 \cdot 10^{0}$	1.00	$2.896 \cdot 10^{-1}$	2.00	$4.500 \cdot 10^{-5}$	2.00	$1.717 \cdot 10^{-2}$	1.00
512	$2.708 \cdot 10^{0}$	1.00	$7.240 \cdot 10^{-2}$	2.00	$1.125 \cdot 10^{-5}$	2.00	$8.586 \cdot 10^{-3}$	1.00
				$\mathbf{E}_h^{0,*}$				
32	$2.175 \cdot 10^{1}$	1.00	$1.848 \cdot 10^{1}$	1.99	$2.494 \cdot 10^{-3}$	1.99	$1.372 \cdot 10^{-1}$	1.00
64	$1.088 \cdot 10^{1}$	1.00	$4.631 \cdot 10^{0}$	2.00	$6.251 \cdot 10^{-4}$	2.00	$6.867 \cdot 10^{-2}$	1.00
128	$5.445 \cdot 10^{0}$	1.00	$1.158 \cdot 10^{0}$	2.00	$1.564 \cdot 10^{-4}$	2.00	$3.434 \cdot 10^{-2}$	1.00
256	$2.723 \cdot 10^{0}$	1.00	$2.896 \cdot 10^{-1}$	2.00	$3.911 \cdot 10^{-5}$	2.00	$1.717 \cdot 10^{-2}$	1.00
512	$1.362 \cdot 10^{0}$	1.00	$7.240 \cdot 10^{-2}$	2.00	$9.778 \cdot 10^{-6}$	2.00	$8.586 \cdot 10^{-3}$	1.00
				$\mathbf{E}_h^{0,*,1}$				
32	$1.267 \cdot 10^{0}$	2.04	$1.848 \cdot 10^{1}$	1.99	$2.309 \cdot 10^{-3}$	1.99	$6.231 \cdot 10^{-3}$	2.00
64	$3.133 \cdot 10^{-1}$	2.02	$4.631 \cdot 10^{0}$	2.00	$5.785 \cdot 10^{-4}$	2.00	$1.555 \cdot 10^{-3}$	2.00
128	$7.796 \cdot 10^{-2}$	2.01	$1.158 \cdot 10^{0}$	2.00	$1.447 \cdot 10^{-4}$	2.00	$3.883 \cdot 10^{-4}$	2.00
256	$1.945 \cdot 10^{-2}$	2.00	$2.896 \cdot 10^{-1}$	2.00	$3.618 \cdot 10^{-5}$	2.00	$9.702 \cdot 10^{-5}$	2.00
512	$4.858 \cdot 10^{-3}$	2.00	$7.240 \cdot 10^{-2}$	2.00	$9.045 \cdot 10^{-6}$	2.00	$2.425 \cdot 10^{-5}$	2.00

Table 5: Convergence results for the lowest order spaces on meshes of trapezoids – compressible regime.

	$\|\boldsymbol{\sigma}-\boldsymbol{\sigma}_h\|$		$\|\mathrm{div}(\boldsymbol{\sigma}-\boldsymbol{\sigma}_h)\|$		$\|\boldsymbol{u}-\boldsymbol{u}_h\|$		$\|r-r_h\|$	
n	error	order	error	order	error	order	error	order
				$\mathbf{E}_h^0$				
32	$5.232 \cdot 10^{1}$	0.85	$8.665 \cdot 10^{1}$	1.02	$8.683 \cdot 10^{-3}$	1.30	$4.740 \cdot 10^{-1}$	0.47
64	$2.769 \cdot 10^{1}$	0.92	$4.318 \cdot 10^{1}$	1.00	$3.546 \cdot 10^{-3}$	1.29	$2.798 \cdot 10^{-1}$	0.76
128	$1.419 \cdot 10^{1}$	0.96	$2.158 \cdot 10^{1}$	1.00	$1.599 \cdot 10^{-3}$	1.15	$1.494 \cdot 10^{-1}$	0.91
256	$7.167 \cdot 10^{0}$	0.98	$1.079 \cdot 10^{1}$	1.00	$7.722 \cdot 10^{-4}$	1.05	$7.668 \cdot 10^{-2}$	0.96
512	$3.600 \cdot 10^{0}$	0.99	$5.392 \cdot 10^{0}$	1.00	$3.824 \cdot 10^{-4}$	1.01	$3.878 \cdot 10^{-2}$	0.98
				$\mathbf{E}_h^{0,*}$				
32	$1.775 \cdot 10^{1}$	1.01	$8.665 \cdot 10^{1}$	1.02	$6.270 \cdot 10^{-3}$	1.11	$1.124 \cdot 10^{-1}$	1.00
64	$8.862 \cdot 10^{0}$	1.00	$4.318 \cdot 10^{1}$	1.00	$3.071 \cdot 10^{-3}$	1.03	$5.623 \cdot 10^{-2}$	1.00
128	$4.428 \cdot 10^{0}$	1.00	$2.158 \cdot 10^{1}$	1.00	$1.527 \cdot 10^{-3}$	1.01	$2.812 \cdot 10^{-2}$	1.00
256	$2.213 \cdot 10^{0}$	1.00	$1.079 \cdot 10^{1}$	1.00	$7.626 \cdot 10^{-4}$	1.00	$1.406 \cdot 10^{-2}$	1.00
512	$1.107 \cdot 10^{0}$	1.00	$5.392 \cdot 10^{0}$	1.00	$3.812 \cdot 10^{-4}$	1.00	$7.029 \cdot 10^{-3}$	1.00
				$\mathbf{E}_h^{0,*,1}$				
32	$1.280 \cdot 10^{0}$	1.98	$8.665 \cdot 10^{1}$	1.02	$6.251 \cdot 10^{-3}$	1.10	$5.531 \cdot 10^{-3}$	1.97
64	$3.222 \cdot 10^{-1}$	1.99	$4.318 \cdot 10^{1}$	1.00	$3.068 \cdot 10^{-3}$	1.03	$1.393 \cdot 10^{-3}$	1.99
128	$8.078 \cdot 10^{-2}$	2.00	$2.158 \cdot 10^{1}$	1.00	$1.527 \cdot 10^{-3}$	1.01	$3.493 \cdot 10^{-4}$	2.00
256	$2.022 \cdot 10^{-2}$	2.00	$1.079 \cdot 10^{1}$	1.00	$7.625 \cdot 10^{-4}$	1.00	$8.745 \cdot 10^{-5}$	2.00
512	$5.059 \cdot 10^{-3}$	2.00	$5.392 \cdot 10^{0}$	1.00	$3.812 \cdot 10^{-4}$	1.00	$2.188 \cdot 10^{-5}$	2.00

7.2. The Quasi-Incompressible Regime

The incompressible elasticity regime is characterized by $\lambda \to \infty$, or, equivalently, $\nu \to 0.5$. In that case the volumetric part of the stress field becomes non-constitutive. It is usually a difficult case to simulate using classical Galerkin approximations (Arnold, 1990). In the stability analysis we proved that the coercivity of the bilinear form $\mathcal{A}(\cdot,\cdot)$ is independent of λ whenever we can take $\boldsymbol{\tau} = \boldsymbol{I}$ in (7a). A similar argument is valid for the finite dimensional case and it is expected that both $\mathcal{RT}-$based and $\mathcal{ABF}-$based approximation spaces with $k \geq 1$ behave well in the quasi-incompressible regime. Therefore, we now show a convergence study based on an example problem by Brenner (1993), where the shear modulus is $\mu = 1.0$ and the function $\boldsymbol{g} = \boldsymbol{g}(x_1, x_2)$ is taken to be as follows:

$$\boldsymbol{g} = \pi^2 \begin{bmatrix} (8\cos(2\pi x_1) - 4)\sin(2\pi x_2) - \cos[\pi(x_1 + x_2)] + \dfrac{2\sin(\pi x_1)\sin(\pi x_2)}{1+\lambda} \\ (4 - 8\cos(2\pi x_2))\sin(2\pi x_1) - \cos[\pi(x_1 + x_2)] + \dfrac{2\sin(\pi x_1)\sin(\pi x_2)}{1+\lambda} \end{bmatrix}.$$

The exact solution $\boldsymbol{u} = \boldsymbol{u}(x_1, x_2)$ is given by

$$\boldsymbol{u} = \begin{bmatrix} (\cos(2\pi x_1) - 1)\sin(2\pi x_2) + \dfrac{\sin(\pi x_1)\sin(\pi x_2)}{1+\lambda} \\ (1 - \cos(2\pi x_2))\sin(2\pi x_1) + \dfrac{\sin(\pi x_1)\sin(\pi x_2)}{1+\lambda} \end{bmatrix}.$$

We use this example to test the behavior of the approximation spaces under both compressible ($\nu = \nu_c = 0.3$) and quasi-incompressible ($\nu = \nu_i = 0.5 - 10^{-7}$) regimes.

Convergence study In this study we only present the results for the trapezoidal mesh. The convergence rates observed in the experiments reflect those obtained in the analysis, confirming that the mixed formulation for the elasticity problem is locking-free with respect to the incompressibility constraint. The results for both the compressible and quasi-incompressible regimes are similar, so we only show the latter (Figure 2). In this experiment, we also show the results for the space

$$\mathbf{E}_h^{0,\#} = (\mathcal{V}_{\mathcal{ABF}}^{0,\#} \times \mathcal{V}_{\mathcal{ABF}}^{0,\#}) \times \mathcal{U}_h^0 \times \mathcal{R}_h^0,$$

with $\mathcal{V}_{\mathcal{ABF}}^{0,\#}$ as defined in (27).

Some observations can be made from these results:

- Elements based on the $\mathcal{R}_h^1$ space for approximating the rotation show similar errors for $\|\boldsymbol{\sigma} - \boldsymbol{\sigma}_h\|$;
- $\mathcal{ABF}_0-$based elements show similar errors for $\|\operatorname{div}\boldsymbol{\sigma} - \operatorname{div}\boldsymbol{\sigma}_h\|$ and $\|\boldsymbol{u} - \boldsymbol{u}_h\|$; these elements share the same space for the approximation of the displacements and the divergence of the stress;
- The error $\|\operatorname{div}\boldsymbol{\sigma} - \operatorname{div}\boldsymbol{\sigma}_h\|$ for $\mathcal{RT}_1-$based spaces is smaller than the one obtained with $\mathcal{ABF}_0-$based spaces, although the convergence rates are similar. We explain this result using a dimension count: the divergence of functions in $\mathcal{ABF}_0-$based spaces is in $\mathcal{P}^0_{\mathcal{ABF}} \times \mathcal{P}^0_{\mathcal{ABF}}$, with each element mapped from $\mathbb{P}_1(\hat{K}, \mathbb{R}^2)$, has dimension 6, while the divergence of $\mathcal{RT}_1-$based is mapped from $\mathbb{P}_{1,1}(\hat{K}, \mathbb{R}^2)$, which has dimension 8.
- In this experiment, the $\mathbf{E}_h^{0,*}$ and $\mathbf{E}_h^{0,\#}$ spaces lead to similar errors.

We highlight that, as expected from the theoretical results, the $\mathcal{RT}_1-$based elements introduced by Arnold et al. (2015) provide $\mathcal{O}(h)$ convergence for $\|\operatorname{div}\boldsymbol{\sigma} - \operatorname{div}\boldsymbol{\sigma}_h\|$, while the $\mathbf{E}_h^1$ elements proposed in this paper provide $\mathcal{O}(h^2)$ convergence for all variables.

Some numerical issues were noted for the quasi-incompressible regime on finer meshes. We impute these issues to errors arising from floating point representation and algebraic operations.

7.3. Errors versus number of equations

We finish this section with the convergence study of the displacement and stress approximations for the test case presented in Section 7.2, on trapezoidal meshes, in terms of the required number of equations to be solved for the use of different compatible spaces. We include the results for the classical Primal Galerkin method, based on finding an H^1-conforming approximation for the displacement field such that the variational form of Equation (4) is satisfied (Arnold, 1990). Such approximation is sought in the finite dimensional subspace

$$Q_k = \left\{ \boldsymbol{w} \in H^1(\Omega, \mathbb{R}^2);\, \boldsymbol{w}|_K \in P_K^0(\mathbb{P}_{k,k}(\hat{K}, \mathbb{R}^2))\ \forall K \in \mathcal{T}_h \right\}, \quad k \geq 1.$$

The stress approximation is then locally computed from (1), on each element $K \in \mathcal{T}_h$:

$$\boldsymbol{\sigma}_h|_K = \boldsymbol{A}^{-1}\boldsymbol{\varepsilon}(\boldsymbol{u}_h|_K).$$

Clearly, stress fields obtained in this fashion will not be $H(\mathrm{div})-$conforming. Component-wise bilinear (Q_1) and biquadratic (Q_2) approximations are compared with the $\mathcal{RT}_1-$based (Arnold et al., 2015) and $\mathcal{ABF}_1-$based ($\mathbf{E}_h^1$) mixed approximations. When the Q_2 space is used, two degrees of freedom (associated to the displacement of the internal node) are statically condensed in each element. The implementation of the mixed formulation is based on the hybrid version described in Section 6, so the only degrees of freedom (DOFs) considered are those associated to the Lagrange multipliers on the edges.

The results for the compressible case shown in Figure 3a indicate that the Primal method based on the Q_2 space leads to the smallest errors in the displacement approximation, for the same number of total degrees of freedom. The approximations based on $\mathbf{E}_h^1$ spaces are as accurate as those of the Primal-Q_2, while the $\mathcal{RT}_1-$based and Primal-Q_1 methods furnish similar errors, considerably greater.

This scenario changes when we analyze the displacement approximation under the quasi-incompressible regime, where the primal method is known for failing. As presented in Figure 3b, the Primal-Q_1 method does not converge while the mixed method with compatible $\mathcal{RT}_1-$based and $\mathbf{E}_h^1$ spaces works well. It is worth noting the high accuracy of the $\mathbf{E}_h^1$ method.

The relevance of the mixed formulation becomes even more clear when we compare the approximation for the stress field (Figure 4): while under the compressible regime the mixed approximations are more accurate than those obtained via post-processing of the primal solution, when the quasi-incompressible regime is considered, the latter strategy is not capable of providing an accurate approximation neither for the stress field nor for its divergence, while the mixed approximation remains viable.

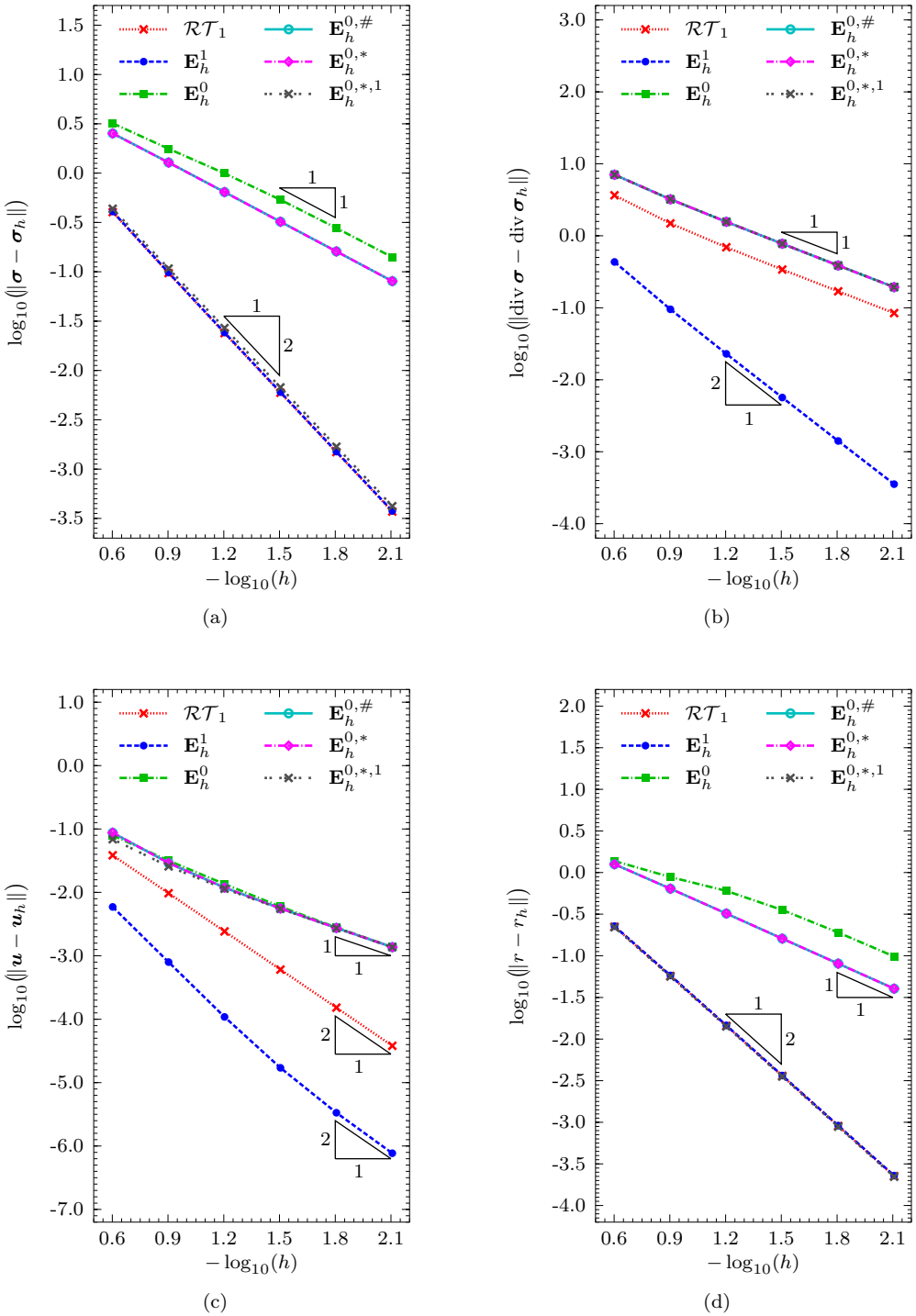

Figure 2: Incompressible case on trapezoidal meshes: convergence results for the approximation using $\mathcal{RT}_1-$based elements, introduced in Arnold et al. (2015), and $\mathcal{ABF}-$based elements. All results for $\mathbf{E}_h^{0,\#}$ and $\mathbf{E}_h^{0,*}$ are similar, so their plots coincide. We can also identify the following similar errors: in (a) and (d), $\mathcal{RT}_1-$based, $\mathbf{E}_h^1$, and $\mathbf{E}_h^{0,*,1}$; in (b) and (c), $\mathbf{E}_h^0$, $\mathbf{E}_h^{0,\#}$, $\mathbf{E}_h^{0,*}$, and $\mathbf{E}_h^{0,*,1}$.

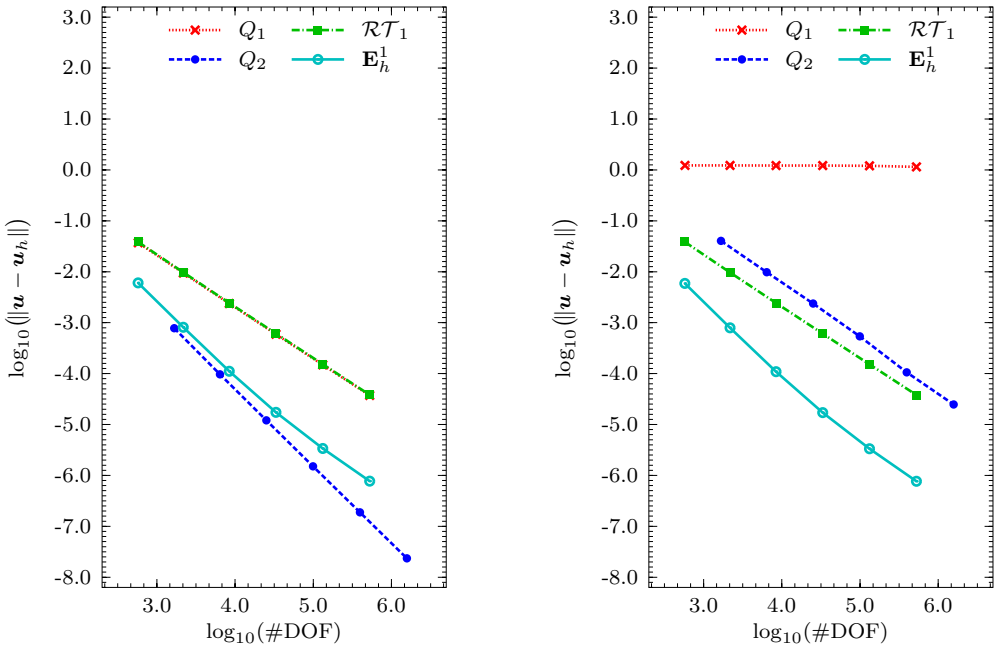

(a) $\nu = \nu_c$ (b) $\nu = \nu_i$

Figure 3: Convergence on trapezoidal meshes of the displacement approximation resulting from the Primal Galerkin method compared with $\mathcal{RT}_1-$based and $\mathbf{E}_h^1$ elements. Compressible (a) and quasi-incompressible (b) regimes.

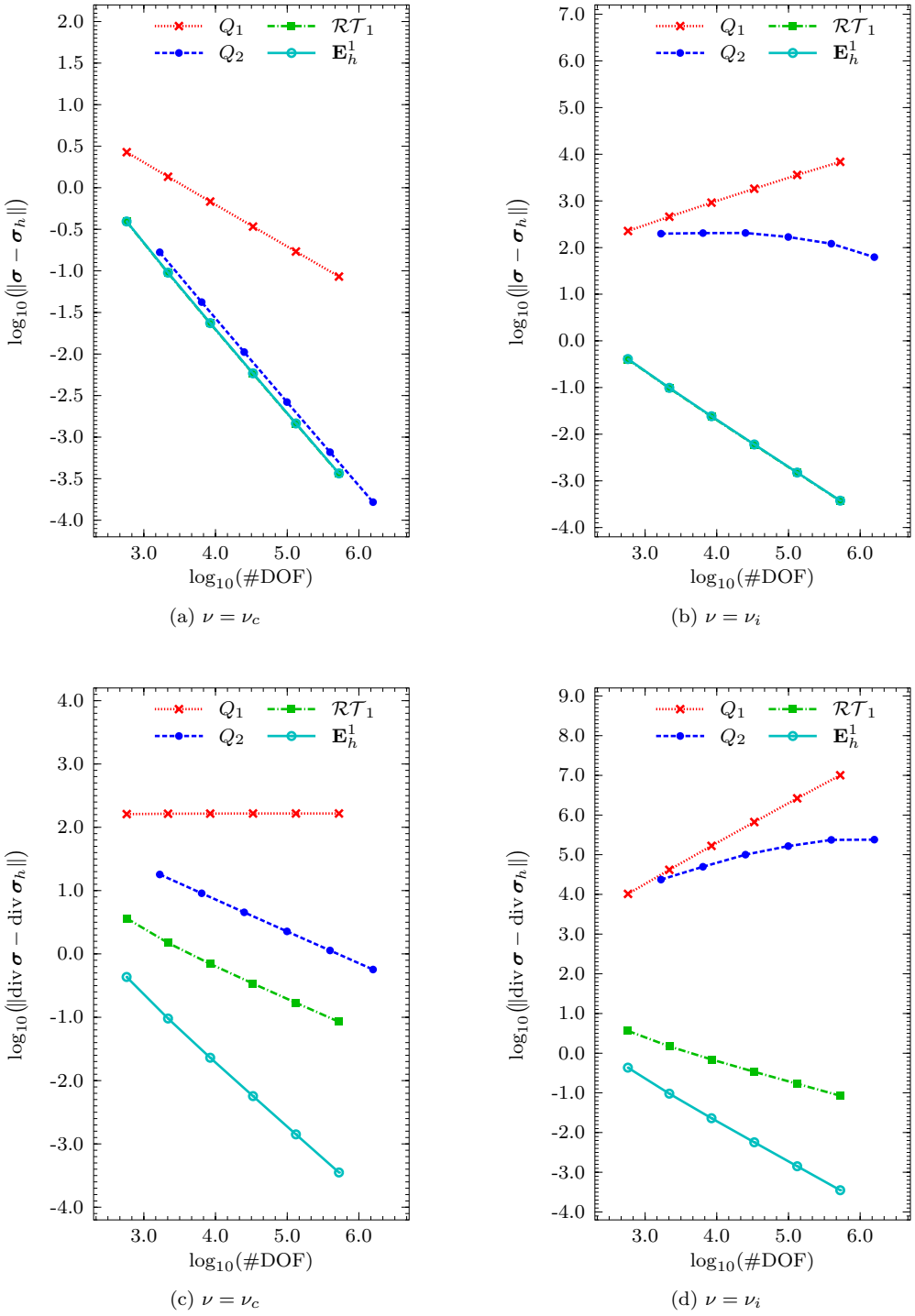

(a) $\nu = \nu_c$ (b) $\nu = \nu_i$

(c) $\nu = \nu_c$ (d) $\nu = \nu_i$

Figure 4: Convergence on trapezoidal meshes of the stress in L^2-norm (first row) and $H(\text{div})-$seminorm (second row). The solution of the Primal Galerkin method is post-processed in each element to obtain an approximation for the stress field that is not $H(\text{div})-$conforming. The error in this approximation is then compared with $\mathcal{RT}_1-$based and $\mathbf{E}_h^1$ elements. Compressible (left column) and quasi-incompressible (right column) regimes. In (a) and (b) the results for $\mathcal{RT}_1-$based and $\mathbf{E}_h^1$ elements are similar.

8. Conclusions

We developed inf-sup stable spaces for the mixed approximation of the linear elasticity problem with variational symmetry of the stress tensor, on convex quadrilateral meshes. These finite elements provide full $H(\mathrm{div})-$approximation of the stress field and the convergence is optimal order for $k \geq 1$. The resulting method is locking-free in the quasi-incompressible regime.

The construction of the elements is based on using $\mathcal{ABF}_k$ spaces for the stress-displacement pair and polynomials of degree k (defined directly on the geometric element) for the rotation. The lowest order case, $k = 0$, requires special treatment: since we could show stability of the natural $\mathcal{ABF}_0-$based spaces only for sufficiently refined meshes, two alternatives were presented, by supplementing the stress-approximating space with divergence-free functions. These enriched spaces have linear normal stresses and are proven to be stable on general quadrilateral meshes. The convergence rates can be improved by approximating the rotation by linear-per-element polynomials. Numerical results confirmed the convergence theory and indicated that a third set of low-order spaces is also possible, although we have no proof that this last choice would be stable in general.

Table 6: Summary of the approximation spaces. The second column indicates whether the elements are affine-mapped from the reference square or are general convex quadrilaterals. The third set of columns gives the expected convergence order ($\mathbf{E}_h^0$ handles quadrilaterals provided h is sufficiently, i.e., extremely, small). Local degrees of freedom are counted per element while the global are counted per edge.

Space	Elements	Convergence Order				DoFs	
		$\boldsymbol{\sigma}$	$\mathrm{div}\,\boldsymbol{\sigma}$	$\boldsymbol{u}$	r	Local	Global
$\mathcal{ABF}-$based							
$\mathbf{E}_h^k, k \geq 1$	Quads	h^{k+1}	h^{k+1}	h^{k+1}	h^{k+1}	$(13k^2+51k)/2+19$	$2k+2$
$\mathbf{E}_h^{0,*,1}$	Quads	h^2	h	h	h^2	31	4
$\mathbf{E}_h^{0,*}$	Quads	h	h	h	h	29	4
$\mathbf{E}_h^0$	Quads	$\to h$	$\to h$	$\to h$	$\to h$	19	2
$\mathcal{RT}_k-$based,	Affine	h^{k+1}	h^{k+1}	h^{k+1}	h^{k+1}	$(13k^2+35k)/2+11$	$2k+2$
$k \geq 1$	Quads	h^{k+1}	h^k	h^{k+1}	h^{k+1}		
$\mathcal{BDM}_1-$based	Affine	h	h	h	h	19	4
	Quads	h	1	h	h		

In every case, the degrees of freedom in the global problem are those corresponding to the traction on edges; the internal degrees of freedom can all be statically condensed and solved for in a set of local problems. This hybrid approach results in a positive-definite global problem and the local problems can be easily solved in parallel. As we have shown in Section 5 the uniform convergence rates are independent of λ, so this result is valid both in compressible and nearly-incompressible regimes.

The convergence order and degree of freedom counting for the proposed spaces are compared with the $\mathcal{RT}_k-$based and $\mathcal{BDM}_1-$based spaces introduced by Arnold et al. (2015) in Table 6.

Acknowledgements

Quinelato acknowledges financial support from CAPES, the Coordination for the Improvement of Higher Education Personnel, Brazil process BEX 6993/15-0 and CNPq, the National Council for Scientific and Technological Development, Brazil grant 141009/2013-6. Loula acknowledges financial support from CNPq grant 312388/2016-0. Correa acknowledges financial support from FAPESP, the Research Foundation of the State of São Paulo, Brazil (Grant 2017/23338-8). Arbogast acknowledges financial support from U.S. National Science Foundation grant DMS-1418752.

Adams, S., & Cockburn, B. (2005). A mixed finite element method for elasticity in three dimensions. *Journal of Scientific Computing*, *25*, 515–521. doi:10.1007/s10915-004-4807-3.

Amara, M., & Thomas, J. M. (1979). Equilibrium finite elements for the linear elastic problem. *Numerische Mathematik*, *33*, 367–383. doi:10.1007/BF01399320.

Arbogast, T., & Correa, M. R. (2016). Two families of $H(\mathrm{div})$ mixed finite elements on quadrilaterals of minimal dimension. *SIAM Journal on Numerical Analysis*, *54*, 3332–3356. doi:10.1137/15M1013705.

Arnold, D. N. (1990). Mixed finite element methods for elliptic problems. *Comput. Methods Appl. Mech. Eng.*, *82*, 281–300. doi:10.1016/0045-7825(90)90168-L.

Arnold, D. N., & Awanou, G. (2005). Rectangular mixed finite elements for elasticity. *Mathematical Models and Methods in Applied Sciences*, *15*, 1417–1429. doi:10.1142/S0218202505000741.

Arnold, D. N., Awanou, G., & Qiu, W. (2015). Mixed finite elements for elasticity on quadrilateral meshes. *Advances in Computational Mathematics*, *41*, 553–572. doi:10.1007/s10444-014-9376-x.

Arnold, D. N., Awanou, G., & Winther, R. (2008). Finite elements for symmetric tensors in three dimensions. *Mathematics of Computation*, *77*, 1229–1251. doi:10.1090/S0025-5718-08-02071-1.

Arnold, D. N., Boffi, D., & Falk, R. S. (2002). Approximation by quadrilateral finite elements. *Mathematics of Computation*, *71*, 909–922. doi:10.1090/S0025-5718-02-01439-4.

Arnold, D. N., Boffi, D., & Falk, R. S. (2005). Quadrilateral $H(\mathrm{div})$ finite elements. *SIAM J. Numer. Anal.*, *42*, 2429–2451. doi:10.1137/S0036142903431924.

Arnold, D. N., Brezzi, F., & Douglas Jr, J. (1984a). PEERS: A new mixed finite element for plane elasticity. *Japan Journal of Applied Mathematics*, *1*, 347–367. doi:10.1007/BF03167064.

Arnold, D. N., Douglas Jr, J., & Gupta, C. P. (1984b). A family of higher order mixed finite element methods for plane elasticity. *Numerische Mathematik*, *45*, 1–22. doi:10.1007/BF01379659.

Arnold, D. N., & Falk, R. S. (1988). A new mixed formulation for elasticity. *Numerische Mathematik*, *53*, 13–30. doi:10.1007/BF01395876.

Arnold, D. N., Falk, R. S., & Winther, R. (2006). Differential complexes and stability of finite element methods II: The elasticity complex. In D. N. Arnold, P. B. Bochev, R. B. Lehoucq, R. A. Nicolaides, & M. Shashkov (Eds.), *Compatible Spatial Discretizations* (pp. 47–67). Springer New York volume 142 of *The IMA Volumes in Mathematics and its Applications*. doi:10.1007/0-387-38034-5_3.

Arnold, D. N., Falk, R. S., & Winther, R. (2007). Mixed finite element methods for linear elasticity with weakly imposed symmetry. *Mathematics of Computation*, *76*, 1699–1723. doi:10.1090/S0025-5718-07-01998-9.

Arnold, D. N., & Winther, R. (2002). Mixed finite elements for elasticity. *Numerische Mathematik*, *92*, 401–419. doi:10.1007/s002110100348.

Arnold, D. N., & Winther, R. (2003). Nonconforming mixed elements for elasticity. *Mathematical Models and Methods in Applied Sciences*, *13*, 295–307. doi:10.1142/S0218202503002507.

Awanou, G. (2009). A rotated nonconforming rectangular mixed element for elasticity. *Calcolo*, *46*, 49–60. doi:10.1007/s10092-009-0159-6.

Boffi, D., Brezzi, F., & Fortin, M. (2009). Reduced symmetry elements in linear elasticity. *Communications on Pure and Applied Analysis*, *8*, 95–121. doi:10.3934/cpaa.2009.8.95.

Boffi, D., Brezzi, F., & Fortin, M. (2013). *Mixed Finite Element Methods and Applications* volume 44 of *Springer Series in Computational Mathematics*. Berlin, Heidelberg: Springer. doi:10.1007/978-3-642-36519-5.

Bramble, J. H., & Hilbert, S. R. (1970). Estimation of linear functionals on Sobolev spaces with application to Fourier transforms and spline interpolation. *SIAM Journal on Numerical Analysis*, *7*, 112–124. doi:10.1137/0707006.

Brenner, S. C. (1993). A nonconforming mixed multigrid method for the pure displacement problem in planar linear elasticity. *SIAM Journal on Numerical Analysis*, *30*, 116–135. doi:10.1137/0730006.

Brezzi, F. (1974). On the existence, uniqueness and approximation of saddle-point problems arising from la-

grangian multipliers. *ESAIM – Modélisation Mathématique et Analyse Numérique*, *8*, 129–151. doi:10.1051/m2an/197408R201291.

Brezzi, F., Douglas Jr, J., & Marini, L. D. (1985). Two families of mixed finite elements for second order elliptic problems. *Numerische Mathematik*, *47*, 217–235. doi:10.1007/BF01389710.

Ciarlet, P. G. (1978). *The Finite Element Method for Elliptic Problems*. Studies in Mathematics and Its Applications. Elsevier Science.

Cockburn, B., Gopalakrishnan, J., & Gusmán, J. (2010). A new elasticity element made for enforcing weak stress symmetry. *Mathematics of Computation*, *79*, 1331–1349. doi:10.1090/S0025-5718-10-02343-4.

Dupont, T., & Scott, R. (1980). Polynomial approximation of functions in Sobolev spaces. *Math. Comp.*, *34*, 441–463. doi:10.1090/S0025-5718-1980-0559195-7.

Farhloul, M., & Fortin, M. (1997). Dual hybrid methods for the elasticity and the Stokes problems: a unified approach. *Numerische Mathematik*, *76*, 419–440. doi:10.1007/s002110050270.

Fraeijs de Veubeke, B. M. (1975). *Stress Function Approach*. Technical Report SA-37 LTAS. URL: http://hdl.handle.net/2268/205875.

Gatica, G. N. (2007). An augmented mixed finite element method for linear elasticity with non-homogeneous Dirichlet conditions. *ETNA. Electronic Transactions on Numerical Analysis*, *26*, 421–438. URL: http://eudml.org/doc/130537.

Gatica, G. N. (2014). *A Simple Introduction to the Mixed Finite Element Method: Theory and Applications*. Springer Briefs in Mathematics. Springer Cham. doi:10.1007/978-3-319-03695-3.

Girault, V., & Raviart, P. A. (1986). *Finite element methods for Navier-Stokes equations: theory and algorithms* volume 5 of *Springer Series in Computational Mathematics*. Springer-Verlag. doi:10.1007/978-3-642-61623-5.

Gopalakrishnan, J., & Guzmán, J. (2011). Symmetric nonconforming mixed finite elements for linear elasticity. *SIAM Journal on Numerical Analysis*, *49*, 1504–1520. doi:10.1137/10080018X.

Gopalakrishnan, J., & Guzmán, J. (2012). A second elasticity element using the matrix bubble. *IMA Journal of Numerical Analysis*, *32*, 352. doi:10.1093/imanum/drq047.

Guzmán, J. (2010). A unified analysis of several mixed methods for elasticity with weak stress symmetry. *Journal of Scientific Computing*, *44*, 156–169. doi:10.1007/s10915-010-9373-2.

Hu, J., & Shi, Z.-C. (2007). Lower order rectangular nonconforming mixed finite elements for plane elasticity. *SIAM Journal on Numerical Analysis*, *46*, 88–102. doi:10.1137/060669681.

Johnson, C., & Mercier, B. (1978). Some equilibrium finite element methods for two-dimensional elasticity problems. *Numerische Mathematik*, *30*, 103–116. doi:10.1007/BF01403910.

Juntunen, M., & Lee, J. (2014). Optimal second order rectangular elasticity elements with weakly symmetric stress. *BIT Numerical Mathematics*, *54*, 425–445. doi:10.1007/s10543-013-0460-2.

Lee, J. J. (2016). Towards a unified analysis of mixed methods for elasticity with weakly symmetric stress. *Advances in Computational Mathematics*, *42*, 361–376. doi:10.1007/s10444-015-9427-y.

Loula, A. F. D., Hughes, T. J. R., Franca, L. P., & Miranda, I. (1987). Mixed Petrov-Galerkin methods for the Timoshenko beam problem. *Computer Methods in Applied Mechanics and Engineering*, *63*, 133–154. doi:10.1016/0045-7825(87)90168-X.

Man, H.-Y., Hu, J., & Shi, Z.-C. (2009). Lower order rectangular nonconforming mixed finite element for the three-dimensional elasticity problem. *Mathematical Models and Methods in Applied Sciences*, *19*, 51–65. doi:10.1142/S0218202509003358.

Mignot, A. L., & Surry, C. (1981). A mixed finite element family in plane elasticity. *Applied Mathematical Modelling*, *5*, 259–262. doi:10.1016/S0307-904X(81)80076-5.

Morley, M. E. (1989). A family of mixed finite elements for linear elasticity. *Numerische Mathematik*, *55*, 633–666. doi:10.1007/BF01389334.

Oyarzúa, R., & Ruiz-Baier, R. (2016). Locking-free finite element methods for poroelasticity. *SIAM Journal on Numerical Analysis*, *54*, 2951–2973. doi:10.1137/15M1050082.

Qiu, W., & Demkowicz, L. (2009). Mixed hp-finite element method for linear elasticity with weakly imposed symmetry. *Computer Methods in Applied Mechanics and Engineering*, *198*, 3682–3701. doi:10.1016/j.cma.2009.07.010.

Raviart, P. A., & Thomas, J. M. (1977). A mixed finite element method for 2-nd order elliptic problems. In I. Galligani, & E. Magenes (Eds.), *Mathematical Aspects of Finite Element Methods* (pp. 292–315). Springer Berlin / Heidelberg volume 606 of *Lecture Notes in Mathematics*. doi:10.1007/BFb0064470.

Stein, E., & Rolfes, R. (1990). Mechanical conditions for stability and optimal convergence of mixed finite elements for linear plane elasticity. *Computer Methods in Applied Mechanics and Engineering*, *84*, 77–95. doi:10.1016/0045-7825(90)90090-9.

Stenberg, R. (1986). On the construction of optimal mixed finite element methods for the linear elasticity problem. *Numerische Mathematik*, *48*, 447–462. doi:10.1007/BF01389651.

Stenberg, R. (1988a). A family of mixed finite elements for the elasticity problem. *Numerische Mathematik*, *53*, 513–538. doi:10.1007/BF01397550.

Stenberg, R. (1988b). Two low-order mixed methods for the elasticity problem. In J. R. Whiteman (Ed.), *The mathematics of finite elements and applications, VI (Uxbridge, 1987)* (pp. 271–280). Academic Press London.

Watwood Jr, V. B., & Hartz, B. J. (1968). An equilibrium stress field model for finite element solutions of two-dimensional elastostatic problems. *International Journal of Solids and Structures*, *4*, 857–873. doi:10.1016/0020-7683(68)90083-8.

Yi, S.-Y. (2005). Nonconforming mixed finite element methods for linear elasticity using rectangular elements in two and three dimensions. *Calcolo*, *42*, 115–133. doi:10.1007/s10092-005-0101-5.

Yi, S.-Y. (2006). A new nonconforming mixed finite element method for linear elasticity. *Mathematical Models and Methods in Applied Sciences*, *16*, 979–999. doi:10.1142/S0218202506001431.

Zienkiewicz, O. C. (2001). Displacement and equilibrium models in the finite element method by B. Fraeijs de Veubeke, Chapter 9, Pages 145–197 of Stress Analysis, Edited by O. C. Zienkiewicz and G. S. Holister, Published by John Wiley & Sons, 1965. *International Journal for Numerical Methods in Engineering*, *52*, 287–342. doi:10.1002/nme.339.